# Coupling the small GTPase Rab3 to the Synaptic Vesicle Cycle

Dissertation Advisor: Prof. Joshua Kaplan Monica Ivelisse Feliu-Mojer

**Coupling the small GTPase Rab3 to the Synaptic Vesicle Cycle**

The small GTPase Rab3 regulates several aspects of neurotransmitter release, such as synaptic vesicle (SV) fusion and release probability, and has been implicated in synaptic plasticity and the regulation of neurotransmitter release by a retrograde synaptic signal. Like all Rab proteins, Rab3 cycles through GTP- and GDP-bound states. Membrane-associated Rab3 binds to its effectors (e.g. RIM) in the GTP-bound state and is extracted from membranes by GDI in the GDP-bound state. This Rab3 cycle occurs in parallel to the SV exo- and endocytosis cycle; however, relatively little is known about how the RAB-3 and SV cycles are coupled.

To address this issue, we used fluorescence recovery after photobleaching (FRAP) of GFP-tagged Rab3, to investigate how SV fusion regulates the dynamic exchange of RAB-3 at *C. elegans* neuromuscular synapses. Photobleaching experiments indicate that 40% of synaptic RAB-3 is mobile. Mobile RAB-3 molecules undergoing dynamic exchange at synapses consist of molecules associated with the plasma membrane (undergoing lateral diffusion), whereas SV-bound RAB-3 molecules are immobile. Mutations disrupting the GTP cycle decrease RAB-3 binding to SVs, thereby diminishing RAB-3's ability to promote exocytosis. Synaptic RAB-3 molecules can exhibit fast or slow mobility. Mutations that block exocytosis dramatically reduce

the rapidly exchanging RAB-3 pool but have little effect on the RAB-3 pool undergoing slow exchange. Interestingly, different exocytic proteins and different RAB-3 effectors promote kinetically distinct forms of RAB-3 exchange. Collectively, our results suggest that synapses contain readily and slowly exchanging pools of RAB-3 and that different modes of exocytosis produce distinct modes of RAB-3 mobility. Our results also suggest a mechanism for how changes in synaptic activity cause changes in the composition of active zones.

**TABLE OF CONTENTS**

## LIST OF FIGURES AND TABLES

**ACKOWLEDGEMENTS**

I would like to begin by thanking Josh Kaplan, for allowing me the freedom to explore my scientific curiosity, and for letting me make my own mistakes and learn from them. Josh has not only supported my academic interests, but he has been very supportive of my non-academic interests, and has encouraged me to keep a healthy life-work balance. Being a student in the Kaplan lab has helped me grow both as a scientist and as a person. I also thank Josh for creating the best and most stimulating work environment I have ever been a part of.

I am incredibly grateful to Jihong Bai, who took me under his wing and was always happy to answer my many questions, even after he moved to Seattle to start his own lab. He is a fantastic mentor, colleague and friend. Jihong taught me so many valuable lessons, from how to do many of the experiments described in this Dissertation, to how to shoot rubber bands to unsuspecting lab mates.

Ed Pym, thank you for instilling some Britishness into this Puerto Rican girl. As the lunchtime enforcer he kept me fed and thus, functional. Ed also turned me to the habit of tea drinking, which I recently discovered was considered a lavish, irresponsible behavior in 19$^{th}$ century. Whatever. Teatime kept me sane, warm and caffeinated. With his straightforward advice, Ed is the best sounding board a graduate student can ask for.

Thank you to Amy Vashlishan-Murray, who together with Ed mentored me through my rotation in the Kaplan Lab and helped me fall in love with *C. elegans*, by

making me poke hundreds of worms a day for three straight weeks. Amy has also been a great example of successful multi-tasking and strength, and a role model.

A big shout out is due to my fellow graduate students. Seungwon (Sebastian) Choi, who was there from Day 1, literally. We started rotating and joined the lab on the same days (within hours of each other) making him kind of my lab twin (sometimes we even dressed the same). Always a great source of advice and conversation, Seungwon also taught me a great deal about hair styling and face moisturizing (insert evil laugh). Katie Thompson-Peer was generous with her time and her advice. Katie made great conversation and was always a willing listener. Her enthusiasm and passion for everything she did was contagious and inspiring. Katie's "radioactiveness" made her so much fun to have around. I would also like to thank the graduate students that preceded me and with whom I briefly overlapped in the lab. Sabrina Hom was a great example of perseverance. David Simon got me interested in RAB-3. Denise Chun was always cheerful and reassuring. All three of them provided me with great insight and advice. A special thank you to former postdoc Kavita Babu, for spreading laughter and joy around, just by being herself. Also, thank you Kavita, for teaching me that tiramisu is always better when it's a little bit frozen.

I'd like to give warm thanks to my baymates for the last two years, Yingsong Hao and Tambu Kudze. Sitting behind me, Yingsong always had my back. She was always encouraging, willing to listen and share her wisdom with me. Tambu arrived as the

quiet and shy new lab technician and it has been a joy to see her funny, sassy and confident side emerge. She is a talented and inspiring young woman.

I'd like to thank Zhitao Hu, the resident electrophysiologist in the lab, for doing some recordings for me. His inhuman efficiency and productivity put us all to shame. That and his ability to nap anywhere is something I hope to replicate someday.

I am grateful for the newest Kaplanites—Dorian "D-train" Anderson, Xia-Jing Tong, Didi Chen, Kelsey Taylor, and Tongtong "TiTi" Zhao—whose arrival has given the lab a boost of fun, energy (mostly due to Dorian) and happiness.

I would like to acknowledge members of the Ruvkun and Ausubel labs, for their generosity and advice. I also acknowledge the administrative and support staff at Molecular Biology, particularly Joanne Desmond.

I am grateful to my Dissertation Advisory Committee members Bernardo Sabatini, Davie Van Vactor, and Tom Rapoport, who always had my best interest in mind, and offered helpful advice about my research, my scientific presentations, and for my career and future. I am thankful to everyone at the Program in Neuroscience, in particular Gary Yellen, Rick Born, Rachel Wilson, former PIN administrator Gina Conquest, and Karen Harmin.

I would like to thank the funding agencies that supported my graduate research. In addition to grants awarded to Josh, my research was supported by the American Psychological Association Minority Fellowship Program and the National Science Foundation Graduate Research Fellowship Program.

I must thank Carlos Jiménez Rivera and Rafael Vázquez Torres, with whom I worked as an undergraduate. Carlos and Rafael gave me the first opportunity to think independently, and explore my capabilities as a scientist. They were always demanding, but loving and encouraging, and frankly made me fall in love with scientific discovery. I also thank Morgan Sheng for allowing me to work in his lab before starting graduate school. My three years in Sheng Lab strongly shaped my scientific interests and prepared me for this journey.

Thank you to the Ciencia Puerto Rico team (Daniel, Giovanna, Wilson, Marcos, Greetchen, Yaihara, Samuel, and Jacky), a dedicated group of people with whom I've had the privilege to volunteer with for the last seven years, promoting science and science education in Puerto Rico. They helped me realize the impact of science beyond the bench and the importance of public engagement with science. Through graduate school, although far from home, the desire to give back to my country and my community has been a guiding light, embodied by this quote from Puerto Rican patriot Pedro Albizu Campos: "*La ley del amor y la ley del sacrificio no admiten la separación. Yo nunca estuve ausente y nunca me he sentido ausente*. (*The law of love and the law of sacrifice do not admit separation. I have never been and have never felt absent*)." Ciencia Puerto Rico has given me and still gives me the opportunity to stay connected, give back, pay it forward and so much more.

Justice Sonia Sotomayor recently wrote: "I have always felt that the support I've drawn from those closest to me has made the decisive difference between success and

failure." So THANK YOU to my dear family, whose unwavering love, support and encouragement have inspired me to strive for success. *Gracias Mami*, for being my friend, my guide and for keeping me grounded. *Gracias Papi*, for instilling in me strength of character, always pushing me to the best that I can be, and for being your unique self. Thank you to my friends, the ones that have always been there in spite of distance and lack of time, and the ones in Boston, who became a family away from my family.

Lastly, thank you to my husband, Luisra. He is the best partner I could have ever hoped for. He has been my friend and accomplice in this adventure called graduate school and many others. His love and support have made me and continue to make me a better person.

*Para mi familia y para Luis Ramón, con todo mi amor*.

# CHAPTER 1

# INTRODUCTION

**Overview of introductory remarks**

Neurotransmitter release is mediated by the exocytosis of synaptic vesicles (SVs) at the presynaptic nerve terminal (Südhof, 2004). Before becoming competent to undergo calcium-evoked fusion, SVs undergo a cycle of highly regulated steps that include synaptic vesicle transport, attachment to the plasma membrane (i.e. docking) and priming. Upon calcium-triggered exocytosis, SVs fuse with the presynaptic plasma membrane and their membrane and associated proteins must be promptly and efficiently retrieved in order to maintain optimal synaptic function. The experiments outlined in this Dissertation investigate the regulation and the coupling of the small GTPase Rab3 to the SV cycle, to better understand how it impacts synaptic transmission. Particularly, this Dissertation focuses on studying the dynamics of RAB-3 at the *C. elegans* neuromuscular synapse. In this introduction, I first briefly discuss synaptic function and the SV cycle. This is followed by an overview of the Rab GTPase cycle, a discussion of the role of Rab3 in neurotransmitter release and the regulation of Rab3 function. Finally, I describe the rationale for studying the dynamics of Rab3 at the synapse and briefly review the main technique we used to do so (i.e. Fluorescence Recovery After Photobleaching or FRAP).

**Brief introduction to synaptic function and the synaptic vesicle (SV) cycle**

The synapse is the fundamental functional unit of the nervous system. Synapses are specialized intercellular junctions, between a presynaptic neuron and a postsynaptic cell (a neuron or muscle), dedicated to the unidirectional flow of chemically encoded information. At the presynaptic nerve terminal, neurotransmitters are packed into synaptic vesicles (SVs) (Südhof, 2012). Upon depolarization of the presynaptic terminal, voltage-gated calcium channels open, letting calcium in, triggering the exocytosis of SVs, which release neurotransmitters into the synaptic cleft, where they activate postsynaptic receptors.

Before becoming competent to undergo calcium-evoked fusion, SVs undergo a trafficking cycle that can be divided into several steps. First, SVs are transported to and cluster around the active zone (AZ), a small electron-dense section of the presynaptic plasma membrane (Südhof, 2012). Synaptic vesicles then attach (i.e. dock) to the plasma membrane, where they are subsequently primed and made competent for calcium-triggered release. Following their fusion to the presynaptic plasma membrane, synaptic vesicles and their components are removed or recycled. The tight regulation of these steps is governed by several evolutionarily conserved proteins and is crucial for producing important synaptic phenomena (Richmond & Broadie, 2002; Südhof, 2004; Südhof & Rizo, 2011; Südhof, 2012; Jahn & Fasshauer, 2012).

Presynaptic nerve terminals are highly dynamic structures dedicated to repeated rounds of SV release. For example, in a central nervous system synapse, there can be

up to 100 fusion events per second (Xue & Mei, 2011). Each SV fusion event presents a challenge to the neuron: every time a synaptic vesicle fuses there is a massive insertion of excess membrane and vesicular proteins into the presynaptic plasma membrane. Thus, each fusion event effectively destabilizes the synaptic structure and to maintain optimal function a synapse must be able to efficiently remove the excess proteins and lipids deposited into the plasma membrane by exocytosis. This not only to prevent complete exhaustion of the limited supply of fusion competent SVs, but to maintain normal presynaptic terminal morphology and availability of release sites (Neher, 2010; Xue & Mei, 2011). Therefore, to sustain continued neurotransmitter release, a synapse must retrieve and recycle these synaptic constituents fast, meaning that the rate at which synaptic proteins are exchanged from the plasma membrane and synaptic vesicles recycled is important for maintaining the fast and precise flow of information that underlies normal brain function. How does a synapse orchestrate such complex membrane trafficking events (i.e. exocytosis, recycling)? How does it regulate the rate of vesicular protein exchange? How does it temporally and spatially regulate the retrieval of material from the plasma membrane upon exocytosis?

**Rab proteins and the GTPase cycle**

The Rab family of small GTPases is the largest subfamily of the Ras superfamily of small GTP-binding proteins, with more than 60 Rab protein genes in mammals, 29 in *Caenorhabditis elegans* and 33 in *Drosophila*. Rab proteins play a critical role in the

temporal and spatial regulation of membrane trafficking events such as vesicle docking, fusion to membranes, and recycling.

Through a GDP/GTP exchange cycle, Rabs function as molecular switches to regulate diverse membrane trafficking events. The activity and association of Rab GTPases with membranes depend upon its bound nucleotide state and are controlled by several regulatory proteins. After being synthesized and prenylated in the cytosol, the cytosolic GDP-bound or “inactive state” Rab associates with GDI (GDP dissociation inhibitor), which inhibits Rabs from releasing GDP (Figure 1.1, Step 1). Prenylation (the addition of lipid tails, illustrated by a pair of angled lines in Figure 1.1, Steps 1 and 3) of Rab proteins makes them competent to associate with membranes (Barrowman & Novick, 2003). Following membrane recruitment, a guanine nucleotide exchange factor (GEF) facilitates the exchange of GDP for GTP (Figure 1.1, Step 2). Activated Rab-GTP can then interact with effector proteins, which act as regulators of the Rab protein pathways (Figure 1.1, Step 3). Stimulation of Rab GTPase activity by a GAP (GTPase activating protein) (Figure 1.1, Step 4) converts the Rab back to its GDP-bound form. GDI retrieves Rab-GDP from membranes to restart the cycle (Figure 1.1, Step 1).

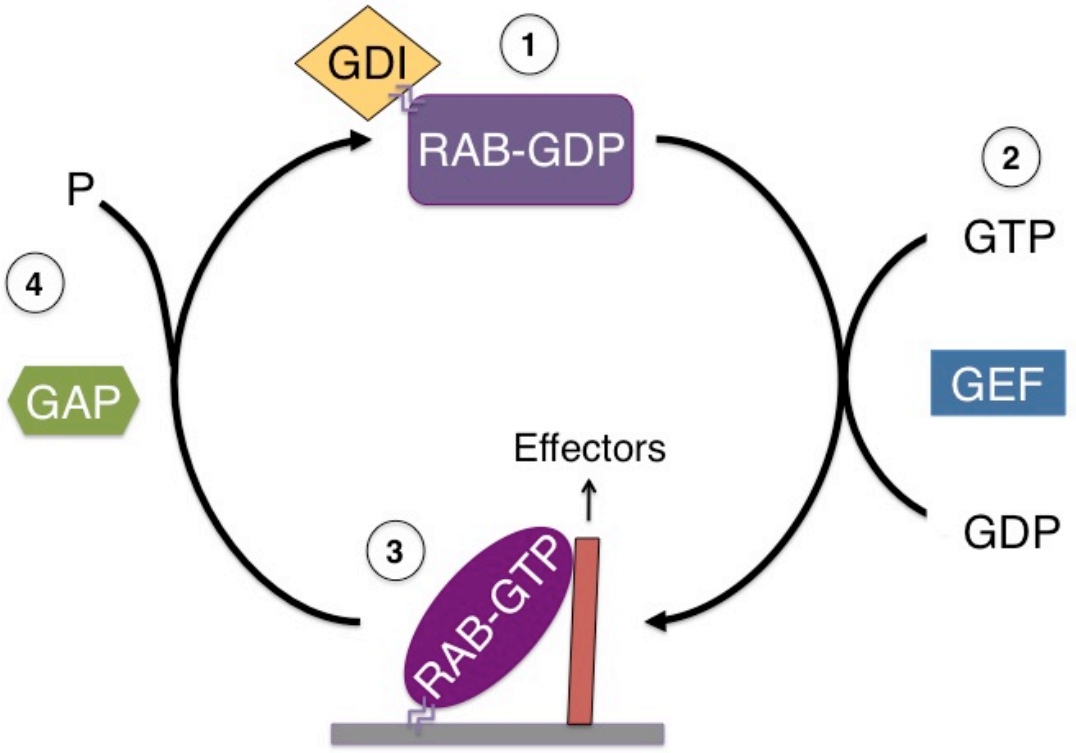


**Figure 1.1 The Rab cycle.** After being synthesized and prenylated in the cytosol, (1) the cytosolic GDP-bound Rab associates with GDI (GDP dissociation inhibitor) (prenyl tails are depicted by a pair of angled lines in Steps 1 and 3). Following membrane recruitment, (2) a guanine nucleotide exchange factor (GEF) facilitates the exchange of GDP for GTP. (3) Activated Rab-GTP can then interact with effector proteins, which act as regulators of the Rab protein pathways. (4) Stimulation of Rab GTPase activity by a GAP (GTPase activating protein) converts Rab back to its GDP-bound form.

Different Rab proteins are found to be specifically associated with distinct subcellular compartments (Zhang et al., 2007). Neurons have specialized membrane trafficking demands and not surprisingly, Rab proteins have an important role in nervous system function. This is evidenced by several hereditary and neurological diseases that

result from the inactivation of *rab* genes and their regulators (Chan et al., 2011). To date, only a small number of Rabs have been shown to associate with SVs. Members of the Rab3 and Rab27 subfamilies are present on synaptic vesicles (SVs) and have been shown to regulate several aspects of vesicle fusion (von Mollard & Mignery, 1990; Mahoney et al., 2006; Moreira et al., 2008). Endosomal Rabs, such as Rab4, Rab5, Rab10, Rab11 and Rab14 have also been identified on SV membranes and are thought to participate in the recycling of SVs (Takamori et al., 2006; Pavlos et al., 2010).

**Regulation of SV fusion by Rab3**

Rab3 is the most abundant Rab small GTPase in neurons and is enriched in synaptic vesicle membranes. Rab3 regulates different aspects of neurotransmitter release. For example, Rab3-deficient mice and worms display reduced excitatory postsynaptic currents (evoked- and mini-EPSCs) (Schlüter et al., 2004; Mahoney, et al., 2006; Simon et al., 2008). In addition, Rab3 and its effector RIM regulate SV release probability after depolarization (Schlüter et al., 2004) and promote SV fusion (Schlüter et al., 2006). Therefore, Rab3 is an intriguing candidate for the normal regulation of evoked neurotransmitter release. Consistent with this, Rab3 has been implicated in mossy fiber and parallel fiber long-term potentiation (LTP) (Castillo et al., 1997; Lonart et al., 1998) and the regulation of neurotransmitter release by retrograde synaptic signals (Simon et al., 2008). Last, Rab3 has been proposed to act on a subset of SVs (Schlüter et al., 2006) to regulate short-term synaptic plasticity. Consistent with this

idea, *C. elegans rab-3* mutants display a depleted population of vesicles at motor neuron synapses, whereas in intersynaptic regions of the axon, vesicle populations are elevated, suggesting that RAB-3 may regulate recruitment of vesicles to the active zone or sequestration of vesicles near release sites (Nonet et al., 1997). More recently, Rab3 was implicated in the regulation of the assembly of the AZ machinery for presynaptic SV release at the *Drosophila* neuromuscular junction (NMJ) (Graf et al., 2009). Thus, by regulating critical parameters for neurotransmitter release and the composition of AZs, Rab3 GTPases could function as biochemical switches that modulate the SV release machinery in an activity-dependent manner. However, the detailed molecular mechanisms of how Rab3 regulates SV release remain elusive.

The GTP-dependent cycle of Rab3 association with donor (i.e. SV) and dissociation from target membranes (i.e. presynaptic plasma membrane) occurs in parallel with the SV cycle (von Mollard et al., 1991). The guanine nucleotide-binding status of Rab3 is modulated by the same regulatory proteins described in the previous section and shown in Figure 1.1. Rab3GEF catalyzes the GDP/GTP exchange that activates Rab3. Rab3 association with SVs requires normal Rab3GEF function (Iwasaki et al., 1997; Mahoney et al., 2006). The hydrolysis of GTP on Rab3 is catalyzed by Rab3GAP, resulting on the removal of Rab3-GDP from membranes by GDI. Consistent with this idea, Rab3GAP deficient mice show accumulation of Rab3-GTP in the brain (Sakane et al., 2006). In yeast and mouse mutants lacking GDI, membrane associated Rab-GDP proteins accumulate (Garrett et al., 1994; D'Adamo et al., 2002).

Nevertheless, several aspects of the Rab3 cycle and how it is coupled to the SV cycle are poorly understood.

**Rab3 effectors**

As a GTP-binding protein, Rab3 acts via its GTP-dependent effectors to exert its action on SV release (Südhof, 2004). In mammals, there are at least two classes of effectors that interact with Rab3-GTP: RIM and Rabphilin. RIMs are active zone proteins, while Rabphilin is a soluble protein that requires Rab3 for binding to SV (Stahl, et al., 1996; Südhof, 2004). A single isoform of RIM (termed UNC-10) and Rabphilin (termed RBF-1) have been found in *C. elegans*. In contrast with mammalian Rabphilin, RBF-1 has been suggested to not act as a RAB-3 effector (Fukuda, 2003; Fukuda et al., 2004). Rabphilin has been described to regulate SNARE function by interacting with SNAP-25 (Staunton et al., 2001; Tsuboi & Fukuda, 2005; Deák et al., 2006). Studies in mice and worms support a role for Rab27 and Rabphilin in the regulation of dense core vesicle (DCV) exocytosis (i.e. neuropeptide release). Via its interaction with Rab27, Rabphilin is important for the localization, tethering and docking of DCVs (Fukuda et al., 2004; Tsuboi & Fukuda, 2006; Feng et al., 2012). However, understanding the role of RBF-1 Rabphilin as a RAB-3 effector and in the regulation of SV exocytosis has remained elusive.

First identified as a Rab3a-interacting molecule, RIM interacts with SV-bound Rab3-GTP and is the primary operator of Rab3 signaling. Genetic, biochemical, and

electrophysiological experiments in invertebrates and vertebrates suggest that RIM has functions beyond being a Rab3 effector. *unc-10* mutants show uncoordinated (UNC) locomotion, have a significant decrease in docked vesicles near the AZ, and a reduction in evoked and spontaneous excitatory postsynaptic currents (EPSCs) at the NMJ (Weimer et al., 2006a; Stigloher et al., 2011). In mice, RIM mutants display a large decrease in synaptic strength, and defects in short-term synaptic plasticity in the CA1 area of the hippocampus and in GABAergic inhibitory synapses. RIM is also necessary for mossy-fiber and cerebellar parallel fiber long-term synaptic plasticity (LTP) (Kaeser & Südhof, 2005). Rab3 has been implicated in the regulation of LTP in these two brain areas, suggesting that RIM acts in LTP via binding to Rab3 (Südhof, 2012).

RIM proteins are central organizers of the presynaptic AZ and they directly or indirectly interact with multiple synaptic proteins. RIM is a multi-domain protein that binds to core AZ proteins such as Munc13, $\alpha$-liprin, ELKS, RIM-binding protein (RIM-BP), Piccolo and Basoon (these last two in vertebrates only) (Südhof, 2012). SV release is tightly regulated by presynaptic proteins and triggered by calcium influx through voltage-gated calcium channels that are close to docked SVs in the AZ. Recently, RIM was shown to regulate the organization and tethering of calcium channels at the presynaptic AZ (Han et al., 2011; Kaeser et al., 2011; Graf et al., 2012).

**Rab3: a molecular switch signaling the arrival of SVs?**

Rab3 and RIM form a tripartite complex with Munc13, a synaptic protein essential for SV priming. Munc13s comprise three brain-expressed isoforms in mammals that are homologues of the *C. elegans* UNC-13, which express two variants in their nervous system (UNC-13 long and UNC-13 short) (Kohn et al., 2000; Südhof, 2012). Mutants lacking UNC-13 have a uniform reduction of docked SVs in the AZ and a decrease in the primed pool of SVs (Richmond et al., 1999). In worms, flies and mice, loss of Munc13 causes an almost complete elimination of synaptic transmission. It is thought that Munc13 regulates priming by unlocking the t-SNARE protein syntaxin to stabilize its open conformation, thus enabling the formation of the trans-SNARE complex that promotes fusion (Richmond & Broadie, 2002). Additional roles for Munc13 have been suggested in docking SVs to the plasma membrane; post-priming activities to promote calcium-evoked fusion (Madison et al., 2005; McEwen et al., 2006); lowering the energy barriers for SV fusion (Basu et al., 2007); and in short- and long-term synaptic plasticity (Rosenmund et al., 2002; Yang & Calakos, 2011).

Individually, the functions of Rab3, RIM and Munc13 have been shown to be important for the regulation of SV release. However, we are only beginning to understand the functional relation between these proteins. Moreover, it remains unclear how their functions are coupled to temporally and spatially regulate the exocytosis of SVs. The functions of RIM and Munc13 are closely related. Worms, mice and flies lacking RIM display synaptic transmission defects similar to those of Munc13 mutants,

albeit less severe. As noted above, Munc13 is proposed to act in SV priming by stabilizing the open conformation of syntaxin. RIM has been suggested to be upstream of the Munc13/syntaxin interaction, and through its interaction with Munc13, to also act as a SV priming factor. Consistent with this idea, the synaptic defects of *unc-10* mutants can be bypassed by the expression of open syntaxin, which also partially rescues the synaptic transmission defects observed in *unc-13* mutants (Koushika et al., 2001). Munc13 forms a homodimer in the absence of RIM, but a heterodimer with it. Recently it has been shown that RIM acts to disinhibit the priming function of Munc13 by disrupting Munc13 homodimerization (Deng et al., 2011). This function is mediated by the N-terminal zinc finger domain of RIM, as expression of the isolated RIM zinc finger is sufficient to activate priming through binding to Munc13 (Deng et al., 2011). Together the results of these studies lead to a model in which the conversion of Munc13 homodimers into RIM/Munc13 heterodimers makes Munc13 competent to interact with syntaxin, enabling it to form SNARE complexes (Südhof, 2012).

What is the role of Rab3 in this complex? Worms, flies and mice mutants for Rab3, RIM and Munc13 show defects in SV docking and/or priming, and synaptic transmission, with Rab3 mutants having the mildest defects and Munc13 the most severe. Mutants for all three proteins also have defects in short- and long-term synaptic plasticity (LTP), with Rab3 and RIM being essential for mossy-fiber LTP (Lonart et al., 1998). Rab3 has been proposed to act as a molecular switch that signals the arrival of a SV to the AZ via its GTP-dependent interaction with RIM. RIM simultaneously binds

to Rab3 and Munc13 via its N-terminal zinc-finger domain (Alam et al., 2005). The Rab3-RIM interaction may signal the arrival of a SV, whereas RIM mediates the monomerization of Munc13 to facilitate the opening of syntaxin via its Munc13 interaction. RIM tethers calcium channels to the AZ, connecting these calcium channels to SVs and other AZ proteins via various binding activities (Kaeser et al., 2011). Collectively, these results lead to a model in which the tripartite complex formed by Rab3/RIM/Munc13 orchestrates the docking and priming of SVs in the AZ (Gracheva et al., 2008). Also, because of their known roles in docking and priming, the regulation of this tripartite complex could provide a biochemical mechanism for modifying synaptic transmission.

**Rab3 dynamics at the synapse**

What happens to Rab3 after SV fusion? Several studies suggest that following synaptic activity, Rab3 dissociates from SVs and diffuses to adjacent non-synaptic axonal regions (Stahl et al., 1994; Star et al., 2005); however, very little is known about the dynamics of Rab3 at the synapse. As mentioned above, in order to sustain high-frequency neurotransmission, presynaptic terminals must constantly exchange the proteins being deposited by exocytosis into the plasma membrane. Thus, the dynamic behavior of synaptic proteins plays an important role in shaping synaptic activity.

The experiments described in Chapter 2 of this Dissertation used Fluorescence Recovery After Photobleaching (FRAP) to investigate the dynamic behavior of RAB-3 at

*C. elegans* neuromuscular synapses, to further understand the coupling of RAB-3 to the SV cycle. FRAP allows for the measurement of the rate at which bleached and unbleached molecules undergo exchange. In a typical FRAP experiment, fluorescent molecules in a small region of interest (ROI) (Figure 1.2, Step 1) are irreversibly photobleached with a focused laser beam (Figure 1.2, Step 2). Subsequently, diffusion of the surrounding unbleached fluorescent molecules into the bleached area leads to the recovery of fluorescence with a particular velocity (Ishikawa-Ankerhold et al., 2012) (Figure 1.2, Step 3). By plotting the fluorescence recovery, one can determine the mobile fraction (the fraction of fluorescent molecules that participate in the exchange) and the immobile fraction (i.e. molecules unable to undergo exchange between bleached and unbleached regions) of the fluorescently-tagged molecule (Figure 1.2, bottom). The speed of fluorescence recovery can also be determined from a photobleaching plot.

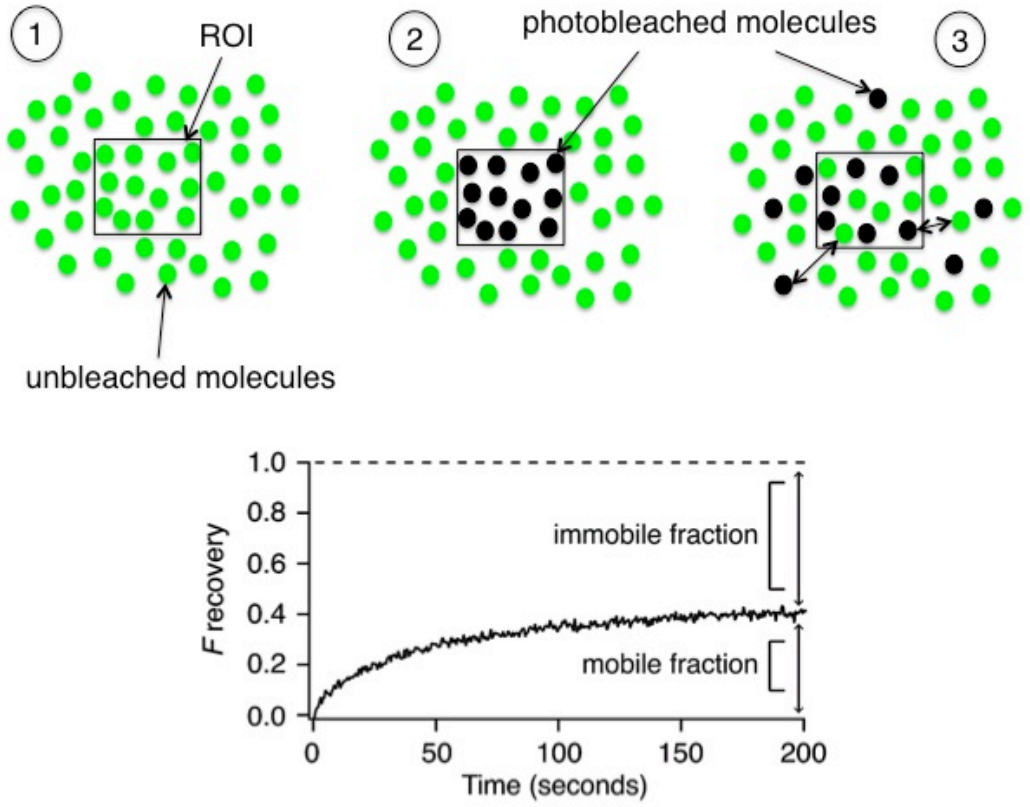


**Figure 1.2 Fluorescence Recovery After Photobleaching (FRAP).** Schematic representation of a FRAP experiment (top) and a fluorescence recovery curve (bottom). (1) A region of interest (ROI) is selected, bleached with a strong laser pulse (2), and the average fluorescence recovery in the ROI is monitored over time (3) (Ishikawa-Ankerhold, et al. 2012). The fluorescence recovery over time can be plotted to determine the mobile and immobile fractions of the fluorescently-tagged molecules (bottom).

# CHAPTER 2

# COUPLING RAB-3 TO THE SYNAPTIC VESICLE (SV) CYCLE

Monica Ivelisse Feliu-Mojer completed all the experiments presented in this chapter, with the exception of the electrophysiological recordings, which were done by Zhitao Hu.

## INTRODUCTION

Neurotransmitter release is mediated by synaptic vesicle (SV) exocytosis at the presynaptic nerve terminal (Südhof, 2004). Several evolutionarily conserved proteins regulate SV docking to the plasma membrane, priming of the fusion machinery, and calcium-evoked fusion. The small GTPase Rab3 regulates different aspects of neurotransmitter release. For example, Rab3-deficient mice and worms display reduced excitatory postsynaptic currents (Schlüter et al., 2004; Simon et al., 2008). In addition, Rab3 and its effector RIM are required for SV docking and the regulation of SV release probability after depolarization (Schlüter et al., 2004) and promote SV fusion (Schlüter et al., 2006). Rab3 has been implicated in short- and long-term potentiation (LTP) (Castillo et al., 1997; Lonart et al., 1998) and the regulation of neurotransmitter release by retrograde synaptic signals (Simon et al., 2008). More recently, Rab3 was implicated in the regulation of the assembly of the AZ machinery for presynaptic SV release at the *Drosophila* neuromuscular junction (NMJ) (Graf et al., 2009).

Like all Rab proteins, RAB-3 cycles through GTP- and GDP-bound states. The Rab3 guanine nucleotide exchange factor (GEF) facilitates the GDP-to-GTP exchange that activates Rab3 and promotes its association with SVs (Iwasaki et al., 1997; Mahoney et al., 2006). Membrane-associated Rab3 binds to its effectors (e.g. RIM) in the GTP-bound state and is extracted from membranes by GDI in the GDP-bound state, after GTP hydrolysis is catalyzed by Rab3GAP (GTPase activating protein) (von Mollard

et al., 1991). This Rab3 cycle occurs in parallel to the SV exo- and endocytosis cycle; yet, very little is known about the coupling of Rab3 to the SV cycle.

Prior studies suggest that SV fusion regulates the mobility of Rab3. Following synaptic activity, Rab3 dissociates from SVs and diffuses to adjacent non-synaptic axonal regions (Stahl et al., 1994; Star, 2005). However, several questions remain about the behavior of Rab3 at the synapse. What are the dynamics of synaptic Rab3? Are the dynamics of Rab3 regulated by exocytosis? To begin addressing these questions, we used fluorescence recovery after photobleaching (FRAP) of GFP-tagged RAB-3, to investigate how SV fusion regulates the dynamic exchange of RAB-3 *C. elegans* neuromuscular synapses.

## RESULTS

### Basic characterization of GFP-tagged RAB-3

To visualize RAB-3 at synapses in intact animals, we expressed GFP-tagged RAB-3 in transgenic animals. Mutants lacking RAB-3 have decreased synaptic transmission, as indicated by resistance to the paralytic effects of aldicarb (an acetylcholine esterase inhibitor), and diminished spontaneous and evoked excitatory postsynaptic currents (EPSCs) in body muscles (Figure 2.1 a-e) (Nonet et al., 1997; Mahoney et al., 2006). Transgenes expressing GFP::RAB-3 in all neurons (using the *snb-1* promoter) rescued the EPSC and aldicarb resistance defects of *rab-3* mutants (Figure 2.1 a-e). Thus, addition of the GFP tag did not impair RAB-3 function.

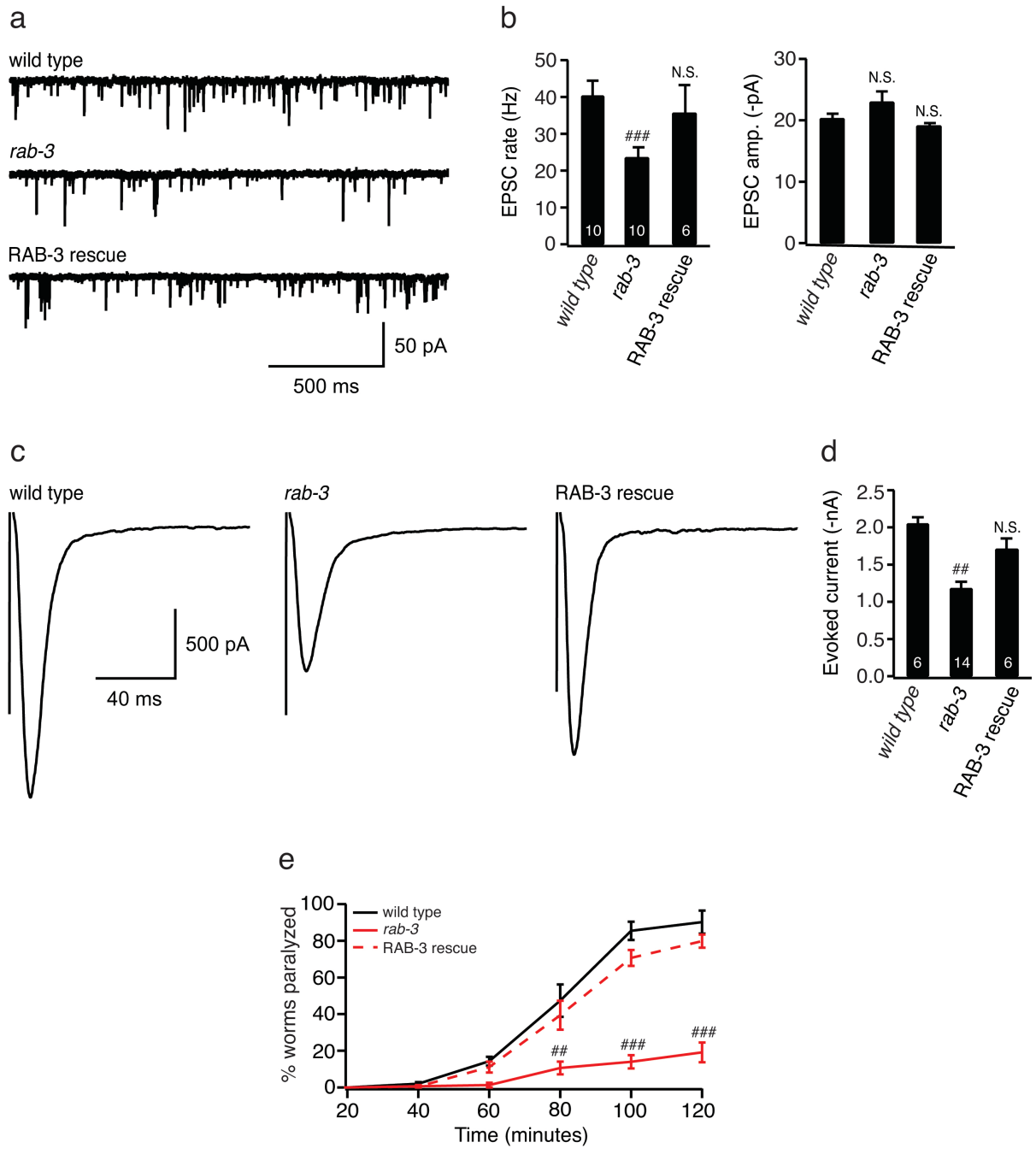


**Figure 2.1 Expression of GFP::RAB-3 rescues synaptic transmission defects in *rab-3* mutants.** (a) Spontaneous and (c) stimulus-evoked EPSCs were recorded from adult body wall muscles of the indicated genotypes. Representative traces of spontaneous EPSCs (a), averaged stimulus-evoked EPSCs (c) and summary data for both are shown (b and d). The number of

***(Continued, Figure 2.1)*** animals analyzed is indicated for each genotype. (e) The paralytic response to aldicarb treatment was analyzed in the indicated genotypes (5-6 trials per genotype, ~25 animals/trial). Statistical significance noted as follows: ##, $p < 0.01$; ###, $p < 0.001$; N.S., not significant, compared to wild type (Student's t-test). Error bars, standard error of the mean (SEM).

To image RAB-3 in identified axons, we expressed GFP::RAB-3 in DA and DB motor neurons (using the *unc-129* promoter). In these motor neurons, GFP::RAB-3 was localized in a punctate distribution in dorsal nerve cord axons (Figure 2.2 a, top image).

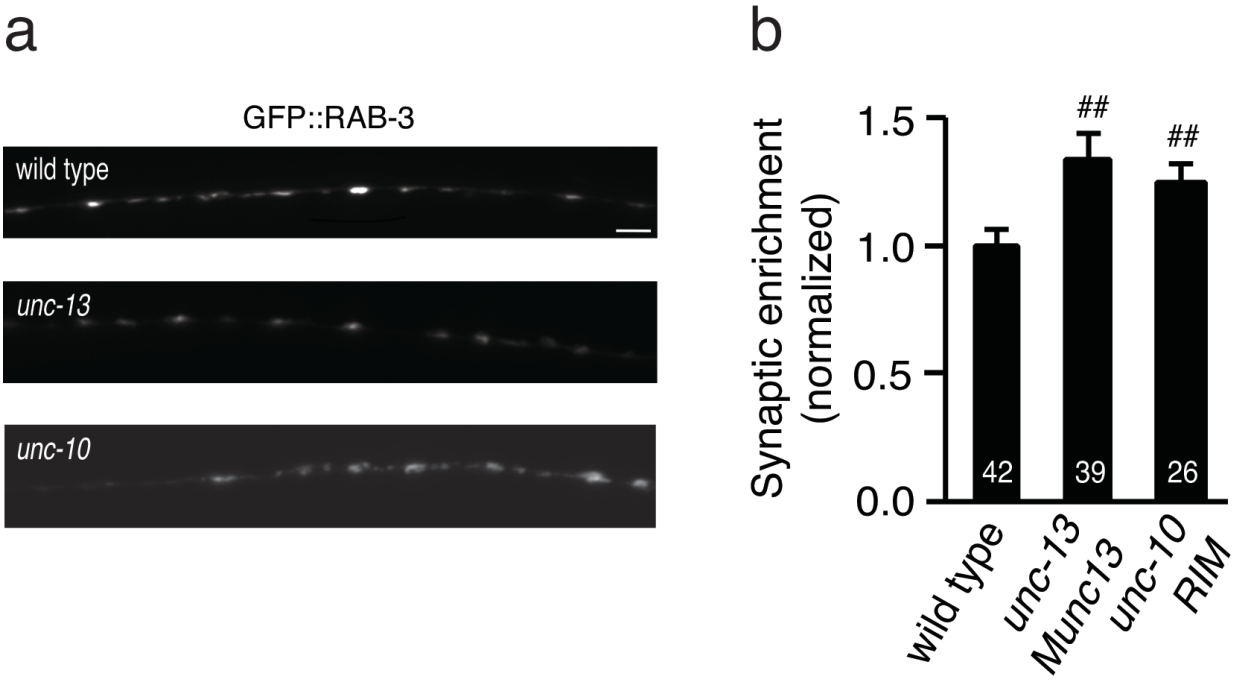


**Figure 2.2 Synaptic RAB-3 is primarily bound to SVs.** (a) Representative images and (b) summary data for GFP::RAB-3 fluorescence in the dorsal nerve cord are shown for wild type, *unc-13* null (*s69* allele) and *unc-10* mutants. The number of worms analyzed for each genotype is indicated. Statistical significance noted as follows: ##, $p < 0.01$, compared to wild type

***(Continued Figure 2.2)*** (Student's t-test). Scale bar, 5 $\mu$m. Error bars, standard error of the mean (SEM).

In addition to the punctate signal, a significant fraction of RAB-3 fluorescence exhibited a diffuse axonal distribution. This diffuse signal likely consists of soluble and plasma membrane associated RAB-3 molecules. To directly assess the abundance of cytoplasmic RAB-3, we analyzed RAB-3 membrane association by subcellular fractionation. The majority of GFP::RAB-3 was associated with membranes in worm extracts (Figure 2.3). The small fraction of RAB-3 that was soluble in biochemical fractionations is unlikely to account for the total diffuse RAB-3 axonal fluorescence. Thus, the majority of the diffuse GFP::RAB-3 signal in axons most likely corresponds to RAB-3 bound to the plasma membrane.

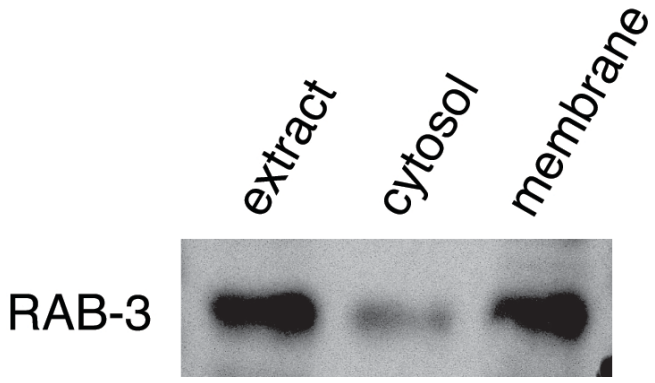


**Figure 2.3 Analysis of RAB-3 membrane association by subcellular fractionation.** Western blots were performed on worm lysates from strains expressing GFP::RAB-3. Rabbit anti-RAB-3 antibody was used.

Many RAB-3 puncta were adjacent to active zones (AZ) (identified with mCherry-tagged ELKS-1) (Figure 2.4), indicating that RAB-3 puncta correspond to pre-synaptic elements.

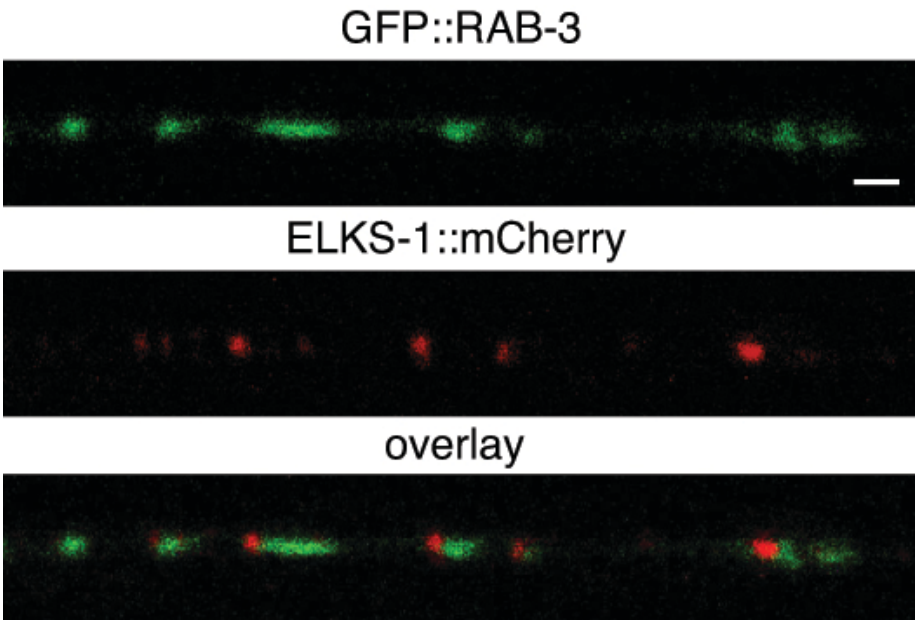


**Figure 2.4 Many RAB-3 puncta are adjacent to active zones (AZ).** GFP::RAB-3 was co-expressed with mCherry-tagged ELKS-1 (an active zone protein) in dorsal axons (using the *unc-129* promoter). Scale bar, 2 $\mu$m.

Prior ultrastructural studies showed that each cholinergic neuromuscular junction (NMJ) contains a single active zone and a pool of ~300 SVs, spanning a domain of approximately 1 μm ( Weimer, 2006b; Hammarlund et al., 2007). Mutations inactivating the anterograde motor UNC-104 KIF1A prevent synaptic localization of RAB-3, implying that the axonal puncta correspond to RAB-3 molecules associated with SVs (Nonet et al., 1997). To further test this idea, we analyzed GFP::RAB-3 distribution in exocytosis

mutants (mEPSC rates: *unc-13* Munc13 0.3% WT; *unc-10* RIM 16% WT). In *unc-13* null and *unc-10* mutants, RAB-3 puncta fluorescence was significantly increased (Figure 2.2 a-b, center and bottom images), consistent with the idea that puncta fluorescence consists primarily of RAB-3 molecules bound to synaptic vesicles (SVs).

**Exocytosis mediates the rapid exchange of SV proteins at presynaptic terminals**

To investigate the dynamic behavior of synaptic proteins, we analyzed their fluorescence recovery after photobleaching (FRAP). FRAP measures the rate at which bleached and unbleached molecules undergo exchange. We performed FRAP experiments on two SV proteins (GFP-tagged SNB-1 Synaptobrevin and RAB-3), both expressed in the DA and DB motor neurons (under the *unc-129* promoter). A single synaptic punctum was photobleached and fluorescence recovery was monitored every 0.5 seconds for 200 seconds (Figure 2.5a). By plotting the fluorescence recovery after photobleaching, we determined the mobile and immobile fractions of each SV protein (Figure 2.5b).

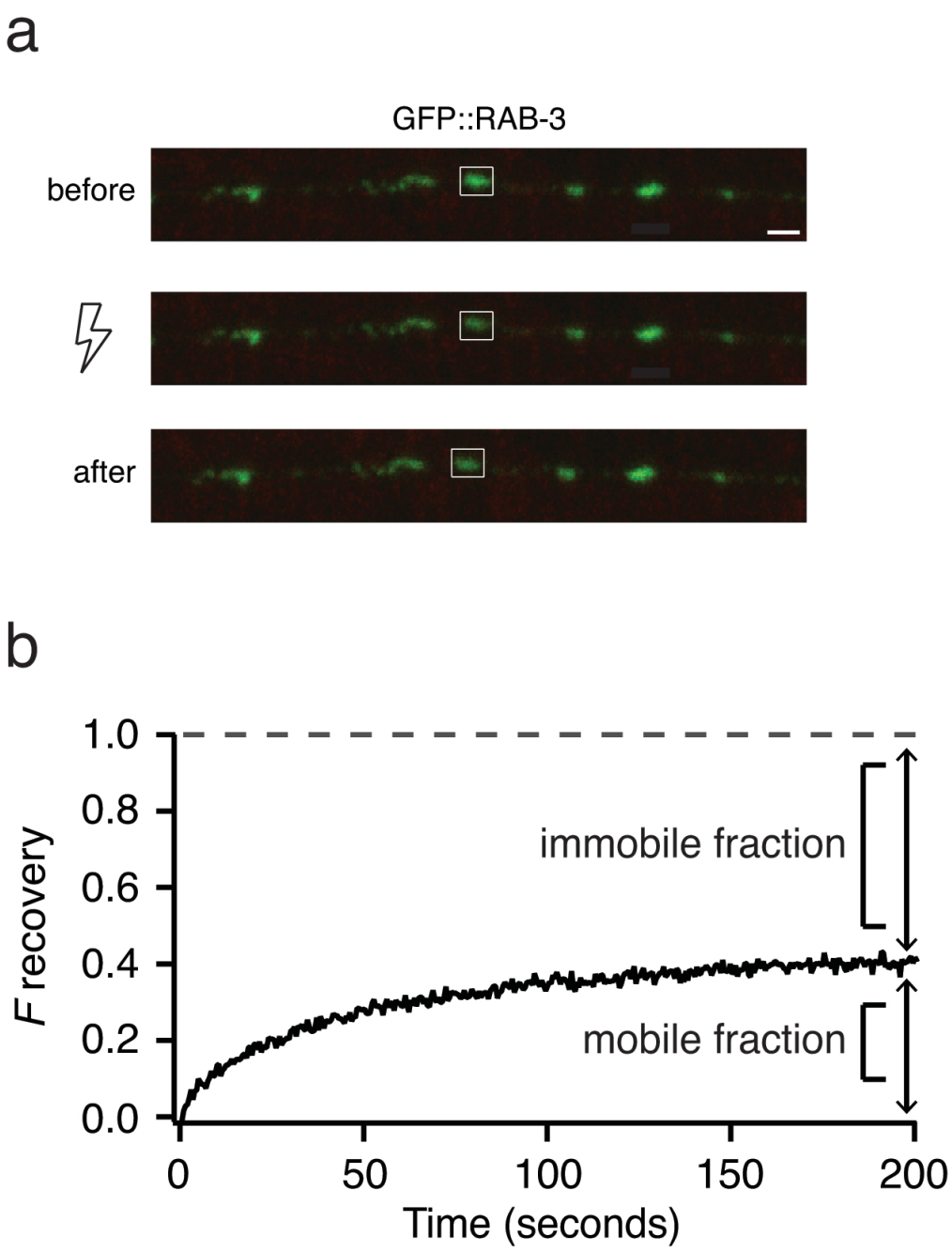


**Figure 2.5 Fluorescence recovery after photobleaching to determine the mobility of SV proteins.** (a) Representative images and (b) average fluorescence recovery curve from a FRAP experiment. Scale bar, 2 $\mu$m.

To determine if fluorescence recovery in a FRAP experiment is mediated by the intrinsic mobility of SVs, we first performed FRAP analysis on GFP::SNB-1. SNB-1 is an integral membrane protein that is highly enriched in SVs. Due to ongoing cycles of SV exo- and endocytosis, SNB-1 equilibrates between the SV pool and the axonal plasma membrane. In FRAP experiments, we found that SNB-1 was relatively immobile and that its mobility was further decreased in *unc-13* mutants (mobile fraction: WT 44%, *unc-13* 29%) (Figure 2.6a). Thus, active exocytosis is required to maintain the mobile pool of SNB-1. Our laboratory previously showed that roughly 30% of SNB-1 resides in the plasma membrane in wild type animals, and that this surface fraction is dramatically reduced in *unc-13* mutants (8% total) (Dittman & Kaplan, 2006). The similar behaviors of mobile and surface SNB-1 suggest that mobile SNB-1 most likely consists of molecules in the plasma membrane undergoing lateral diffusion and that SVs are relatively immobile at these synapses.

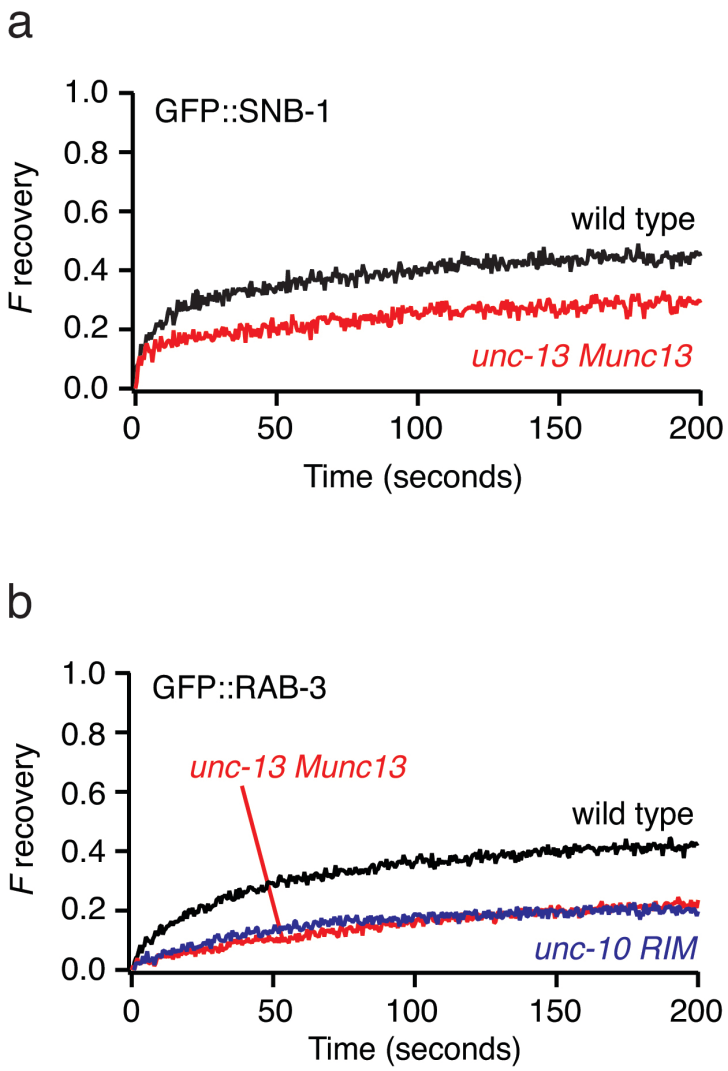


**Figure 2.6 SV proteins are delivered to the plasma membrane by exocytosis.** Average fluorescence recovery curves of (a) GFP::SNB-1 and (b) GFP::RAB-3 in the indicated genotypes.

Membrane bound RAB-3 molecules should also equilibrate between SVs and the plasma membrane. Given the SNB-1 results, we expect that RAB-3 molecules associated with SVs would also be immobile. Photobleaching experiments indicate that 44% of RAB-3 is mobile (Figure 2.6b, black trace). RAB-3 mobility was further reduced

in both *unc-13* and *unc-10* mutants (Figure 2.6b, red and blue traces, respectively). Thus, the majority of RAB-3 puncta fluorescence was immobile and most likely consists of RAB-3 molecules associated with SVs. Assuming that cytoplasmic RAB-3 diffuses at a rate similar to soluble GFP, cytoplasmic RAB-3 fluorescence would be fully recovered at the first time point following photobleaching (i.e. at 0.5 seconds). Consequently, cytoplasmic RAB-3 molecules are unlikely to mediate the fluorescence recovery we observed on a time scale of 10's of seconds. These results indicate that mobile RAB-3 molecules undergoing dynamic exchange at synapses are provided by SV exocytosis, and likely consist of molecules associated with the plasma membrane (i.e. after SV fusion).

Although RAB-3 mobility was reduced, significant fluorescence recovery still occurred in both *unc-13* and *unc-10* mutants. Thus, a substantial fraction of RAB-3 exchange at synapses is mediated by a process that does not require SV exocytosis. To isolate the exocytosis-dependent component of RAB-3 recovery, we subtracted the RAB-3 recovery observed in *unc-13* mutants (Figure 2.7a, red trace) from that in wild type animals (Figure 2.7a, black trace; subtraction is in grey). This analysis suggests that ~90% of the UNC-13-dependent recovery occurred at 50 seconds after photobleaching (Figure 2.7a, indicated with black dashed line). After 50 seconds, the remaining slow component of fluorescence recovery was mediated by an exocytosis-independent process (i.e. that does not require UNC-13). Consequently, to estimate the

RAB-3 exchange that is mediated by SV exocytosis, hereafter we report RAB-3 fluorescence recovery at the 50 seconds time point (Figure 2.7b).

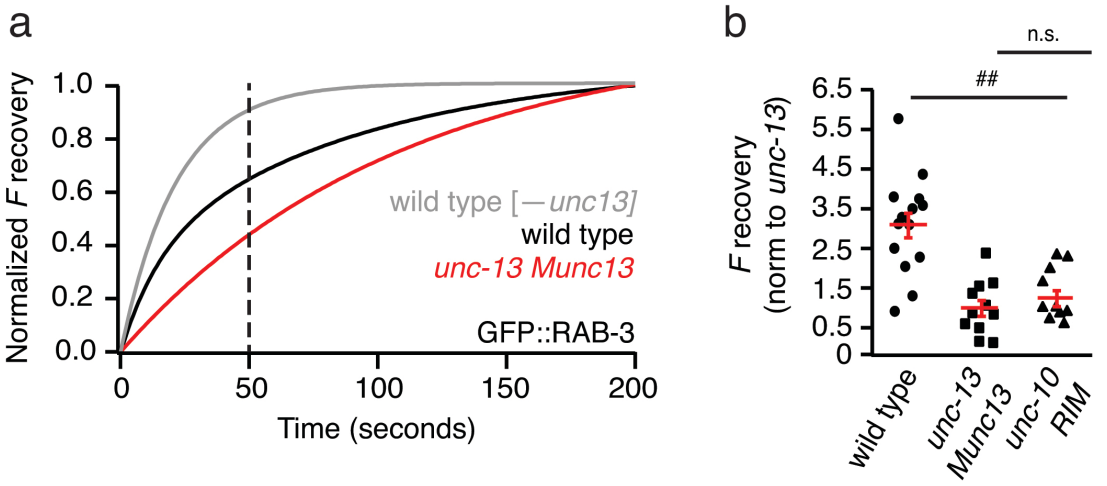


**Figure 2.7 Rapid exchange of RAB-3 at synapses is mediated by exocytosis**. (a) To isolate the exocytosis-dependent component of RAB-3 recovery, we subtracted the RAB-3 recovery observed in *unc-13* mutants (red) from that in wild type animals (black; subtraction in grey). Our analysis suggests that most of theexocytosis-dependent recovery occurred at 50 seconds after photobleaching (dashed line). Fitted recovery curves are shown. (b) Magnitude of RAB-3 fluorescence recovery (normalized to *unc-13*) at the 50 seconds time point in the indicated genotypes. Statistical significance noted as follows: ##, $p < 0.01$, compared to wild type; n.s., not significant, compared to *unc-13* (Student's t-test). Error bars, standard error of the mean (SEM).

Next, we analyzed the kinetics of RAB-3 exchange. In wild type animals, RAB-3 recovery was biexponential ($\tau_{fast}$=8.5s, amplitude=30%; $\tau_{slow}$=79s, amplitude=70%) (Figure 2.8a, black trace; Figure 2.8b and data not shown). In all other genotypes, RAB-3 recovery was well described as a single exponential. Mutations decreasing SV

exocytosis consistently reduced both the magnitude and rate of RAB-3 recovery. To illustrate the relationship between RAB-3 FRAP and exocytosis, we plotted the magnitude (*F* recovery) and speed ($\tau$) of RAB-3 recovery versus the spontaneous EPSC rate (an estimate of SV fusion rate) for several genotypes [*unc-13* null, *unc-13(e1091)*, *unc-13s*, *unc-10*, *rbf-1* and *tom-1*]. For this analysis, we utilized the fast component ($\tau_{fast}$) of RAB-3 exchange for wild type animals because the exocytosis-independent process most likely accounts for a large fraction of the slow component, due to their similar kinetics (WT $\tau_{slow}$=79s, *unc-13* $\tau$=114s). Both the magnitude and speed of RAB-3 exchange at synapses were strongly correlated with the exocytosis rate (correlation with mEPSC rate: *F* recovery, r=0.97, $p<0.001$; $\tau$, r=-0.877, $p<0.05$) (Figure 2.8 c-d). Collectively, these results suggest that the rapid component of RAB-3 exchange at synapses is mediated by SV exocytosis.

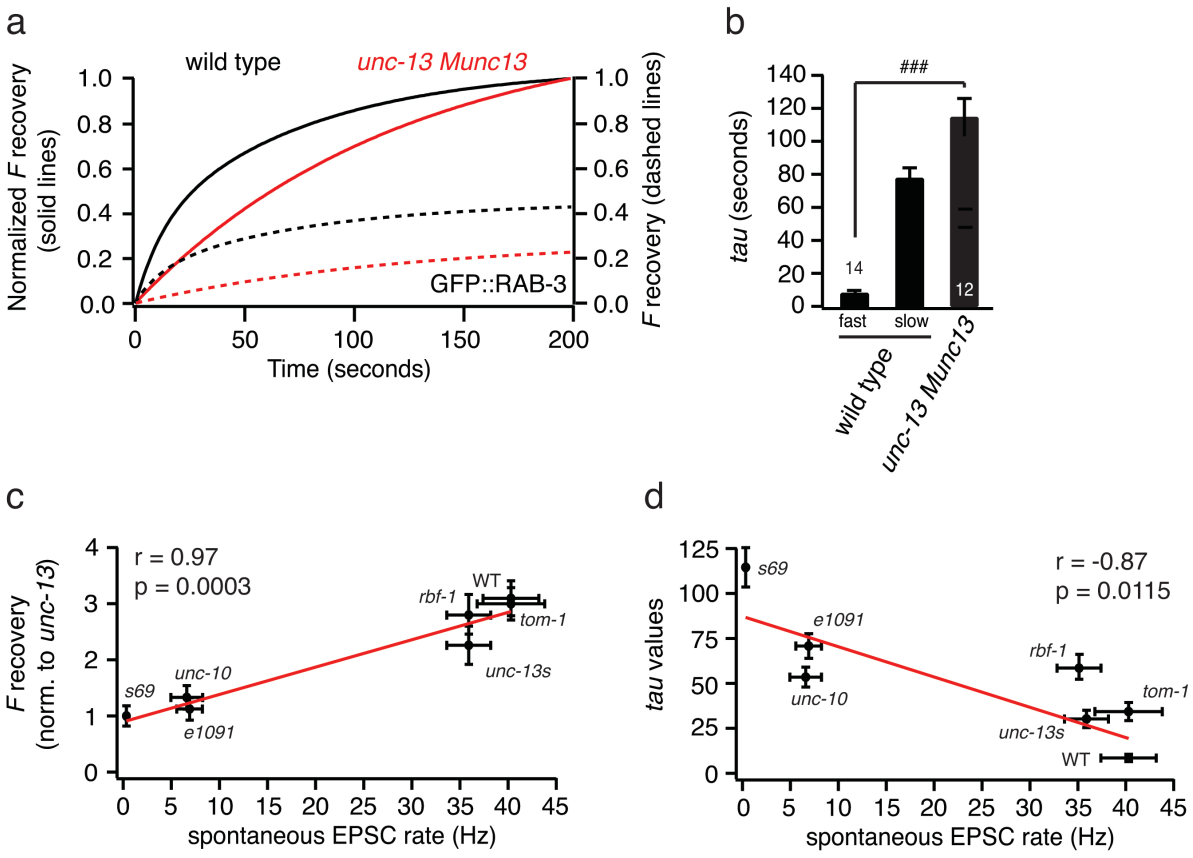


**Figure 2.8 Magnitude and speed of RAB-3 exchange at synapses strongly correlates with the exocytosis rate.** (a) GFP::RAB-3 fitted average fluorescence recovery curves in wild type and *unc-13* null mutants (dashed lines, right axis). Fitted normalized fluorescence recovery curves are also shown (solid lines, left axis). (b) Tau (τ) values for the kinetic components of RAB-3 exchange in wild type and *unc-13* null mutants. The number of worms analyzed for each genotype is indicated. (c) Correlation plots comparing the magnitude (*F* recovery, normalized to *unc-13* null values) and (d) speed (tau,τ) of RAB-3 recovery versus the spontaneous EPSC rate (an estimate of SV fusion rate) in several genotypes. **Wild type**: *F* recovery=3.09, $\tau_{fast}$=8.5s, mEPSC=40.3 Hz; ***unc-13* null**: *F* recovery=1, τ=114s, mEPSC=0.33 Hz; ***unc-13(e1091)***: *F* recovery=1.13, τ=71s, mEPSC=6.9 Hz; ***unc-13s***: *F* recovery=2.26, τ=30s, mEPSC=35.9 Hz; ***unc-10***: *F* recovery=1.33, τ=53s, mEPSC=6.6 Hz; ***tom-1***: *F* recovery=2.99, τ=34s, mEPSC=40.3

***(Continued, Figure 2.8)*** Hz; ***rbf-1***: *F* recovery=2.73, τ=61s, mEPSC=35 Hz. Error bars, standard error of the mean (SEM).

**Different modes of exocytosis produce different rates of RAB-3 exchange**

The preceding results suggest that RAB-3 molecules associated with the plasma membrane are mobile and that several kinetically distinct processes mediate RAB-3 exchange at synapses. What accounts for these distinct modes of RAB-3 recovery? As a GTP-binding protein, RAB-3 acts via its GTP-dependent effectors to exert its action on SV release (Staunton et al., 2001; Sudhof, 2004; Gracheva at al., 2008). Thus binding of RAB-3 to different effectors may affect RAB-3 dynamics. In mammals there are at least two classes of effectors that interact with Rab3-GTP: RIM and Rabphilin. RIM is a key active zone protein and is the best characterized Rab3 effector (Okamoto et al., 1997; Kaeser & Südhof, 2005; Gracheva et al., 2008; Han et al., 2011; Kaeser et al., 2011). Rabphilin is a soluble protein that requires Rab3 for binding to SVs (Stahl, et al., 1996; Südhof, 2004). We analyzed RAB-3 fluorescence recovery in mutants for both RBF-1 Rabphilin and UNC-10 RIM. Inactivating RBF-1 had no effect on mEPSC rate but significantly slowed RAB-3 recovery (WT τ=8.5s, *rbf-1* τ=60s; Figure 2.9a and 2.9e). *unc-10* mutants have significant exocytosis defects and a corresponding decrease in the magnitude of RAB-3 fluorescence recovery (Figure 2.8c and 2.9d). Because rapid RAB-3 exchange and exocytosis rate are tightly correlated (Figure 2.8 c-d), we analyzed the effects of specific exocytic proteins on RAB-3 exchange by comparing mutants that have similar exocytosis rates. Thus, to control for the exocytosis defect in *unc-10*

mutants, we looked at RAB-3 recovery in an *unc-13* allele that displays synaptic defects similar to *unc-10* mutants. The *unc-13* gene contains two promoters. The upstream promoter expresses UNC-13L (Long), while the downstream promoter (which lies in the intron between exons 13 and 14 of the *unc-13L* cistron) expresses UNC-13S (Short) (Kohn et al., 2000). UNC-13L's C2a domain binds directly to UNC-10 RIM; consequently, we expect similar synaptic defects in *unc-13(e1091)* and *unc-10* RIM mutants. Consistent with this idea, *unc-13(e1091)* and *unc-10* mutants had indistinguishable mEPSC rates, yet there was a trend indicating slightly faster RAB-3 recovery in *unc-10* mutants [*unc-10* $\tau$=53s, *unc-13(e1091)* $\tau$=71s, p=0.06; Figure 2.8 c-d and Figure 2.9 b-c and e]. Although this difference was not significant, this result suggests that binding to UNC-10 may confine RAB-3 exchange at synapses. Thus, two putative RAB-3 effectors had opposite effects on RAB-3 exchange kinetics.

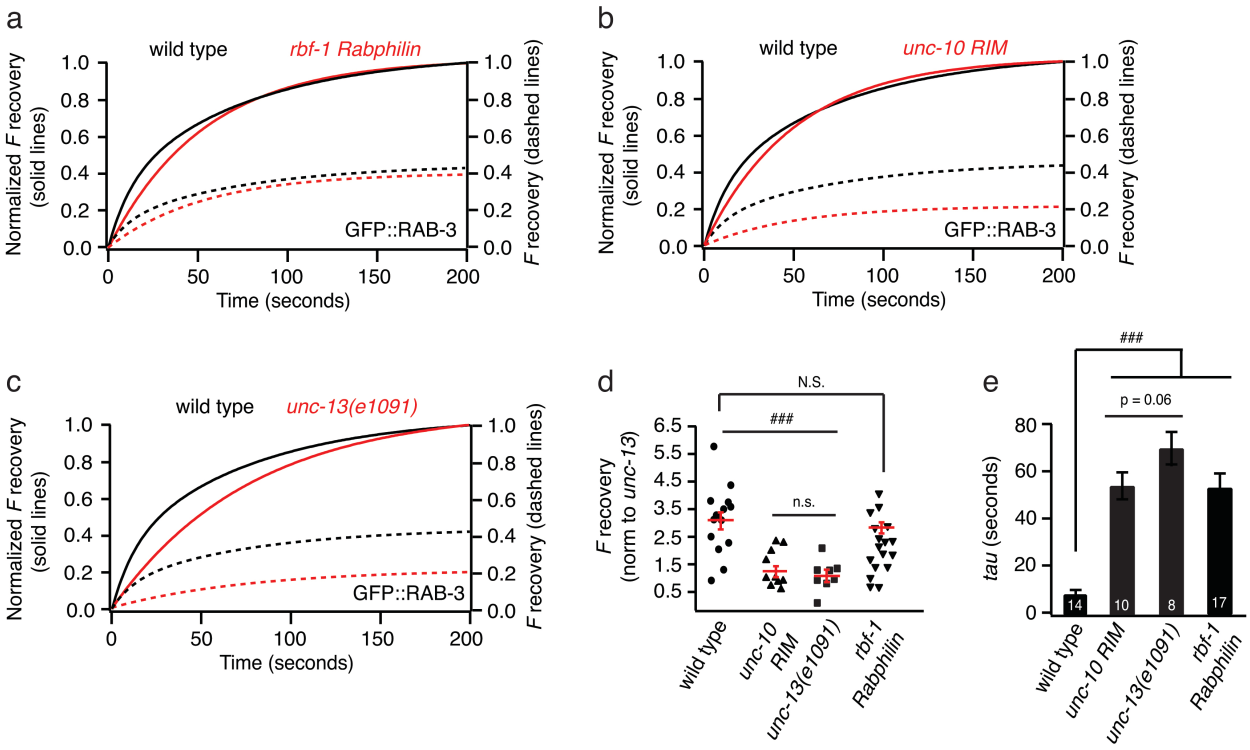


**Figure 2.9 Two putative RAB-3 effectors have opposite effects on RAB-3 exchange kinetics.** (a-c) GFP::RAB-3 fitted average fluorescence recovery curves in the indicated genotypes (dashed lines, right axis). Fitted normalized fluorescence recovery curves are also shown (solid lines, left axis). (d) Magnitude of RAB-3 fluorescence recovery (normalized to *unc-13*) at the 50 seconds time point in the indicated genotypes. (e) Tau (τ) values for the kinetic components of RAB-3 recovery in wild type, *unc-10*, *unc-13(e1091)* and *rbf-1* mutants (only $\tau_{fast}$ is shown for wild type). Statistical significance noted as follows: ###, $p < 0.001$; N.S., not significant, compared to wild type; n.s., compared to *unc-10* (Student's t-test). The number of worms analyzed for each genotype is indicated. Error bars, standard error of the mean (SEM).

At most synapses, neurotransmitter release is comprised by different modes of exocytosis, regulated by different exocytic proteins. Results from our laboratory (Hu et

al., unpublished) indicate that UNC-13 Long (UNC-13L) and the syntaxin-binding protein TOM-1 Tomosyn are involved in the regulation of independent SV exocytosis mechanisms that operate in parallel. Mutants lacking UNC-13S (i.e. UNC-13L rescue) and those lacking TOM-1 Tomosyn had wild type mEPSC rates, yet RAB-3 recovery was significantly slower, indicating that these proteins accelerate exchange of synaptic RAB-3 (Figure 2.10).

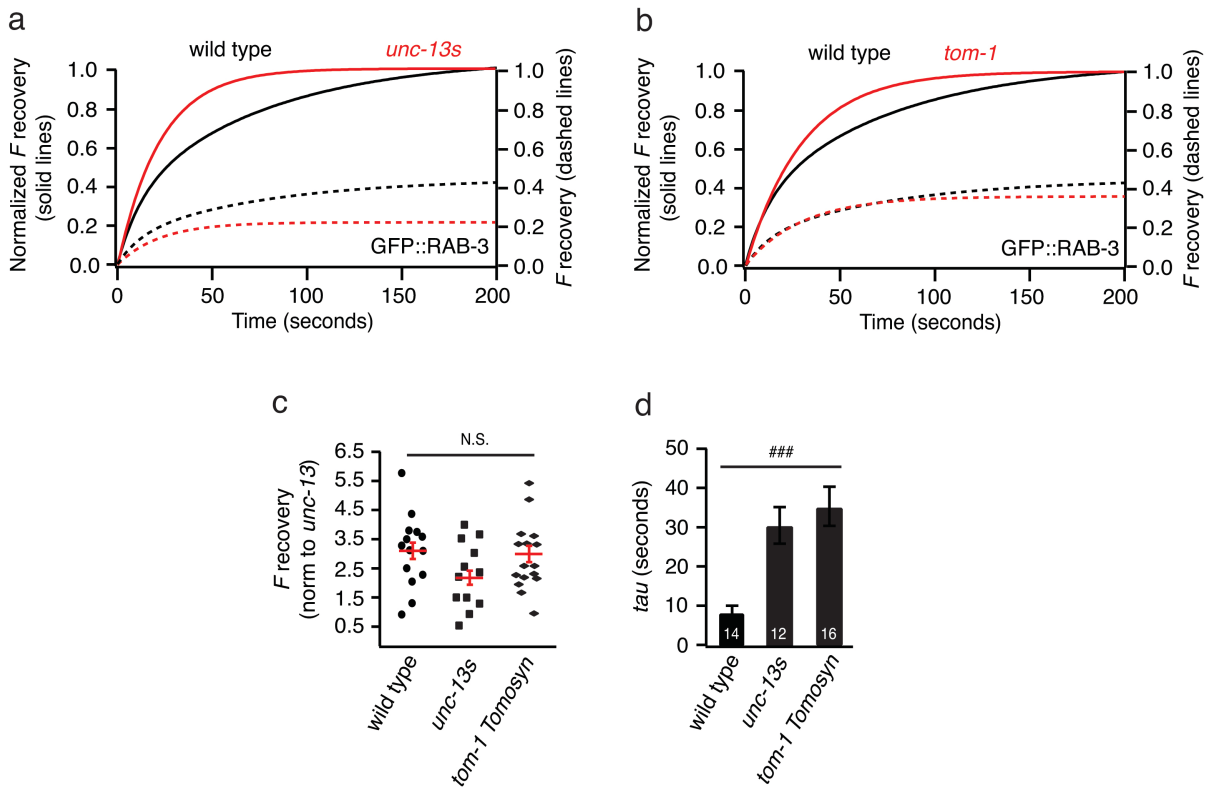


**Figure 2.10 Inactivation of UNC-13S and TOM-1 slow down RAB-3 recovery.** (a-b) GFP::RAB-3 fitted average fluorescence recovery curves in *unc-13s* and *tom-1* mutants (dashed lines, right axis). Fitted normalized fluorescence recovery curves are also shown (solid lines, left axis). (c) Magnitude of RAB-3 fluorescence recovery (normalized to *unc-13*) at the 50 seconds

***(Continued, Figure 2.10)*** time point in the indicated genotypes. (d) Tau ($\tau$) values for the kinetic components of RAB-3 recovery in wild type, *unc-13s* and *tom-1* mutants (only $\tau_{fast}$ is shown for wild type). Statistical significance noted as follows: ###, $p < 0.001$; N.S., not significant, compared to wild type (Student's t-test). The number of worms analyzed for each genotype is indicated. Error bars, standard error of the mean (SEM).

Neurons secrete neuropeptides via the exocytosis of dense core vesicles (DCVs). In contrast to small clear SVs, DCVs are not localized at synaptic zones, but are more diffusely scattered around the nerve terminal (Weimer et al., 2006). RAB-3 likely associates with multiple classes of exocytic organelles; consequently, the dynamic behavior of RAB-3 in the plasma membrane may differ depending on which organelle fused. To test if DCV exocytosis has a role in delivering RAB-3 to the plasma membrane we analyzed RAB-3 recovery in *ric-7* mutants, which are deficient for DCV exocytosis but have wild type mEPSC rates (Hao et al., 2012). In *ric-7* mutants, the magnitude and rate of RAB-3 mobility were not significantly altered ($\tau_{fast}$: WT 8.5s, amplitude=30%; *ric-7* 5.6s, amplitude=25%, p=0.26, Figure 2.11b-c), indicating that DCV exocytosis probably does not play a significant role in delivering RAB-3 to the plasma membrane. Collectively, these results suggest that the amount of RAB-3 available for rapid exchange (i.e. occurring in 10's of seconds) is determined by exocytosis rate and that RAB-3's exchange kinetics in the plasma membrane differs depending on which effectors RAB-3 binds to and which proteins mediated an exocytosis event.

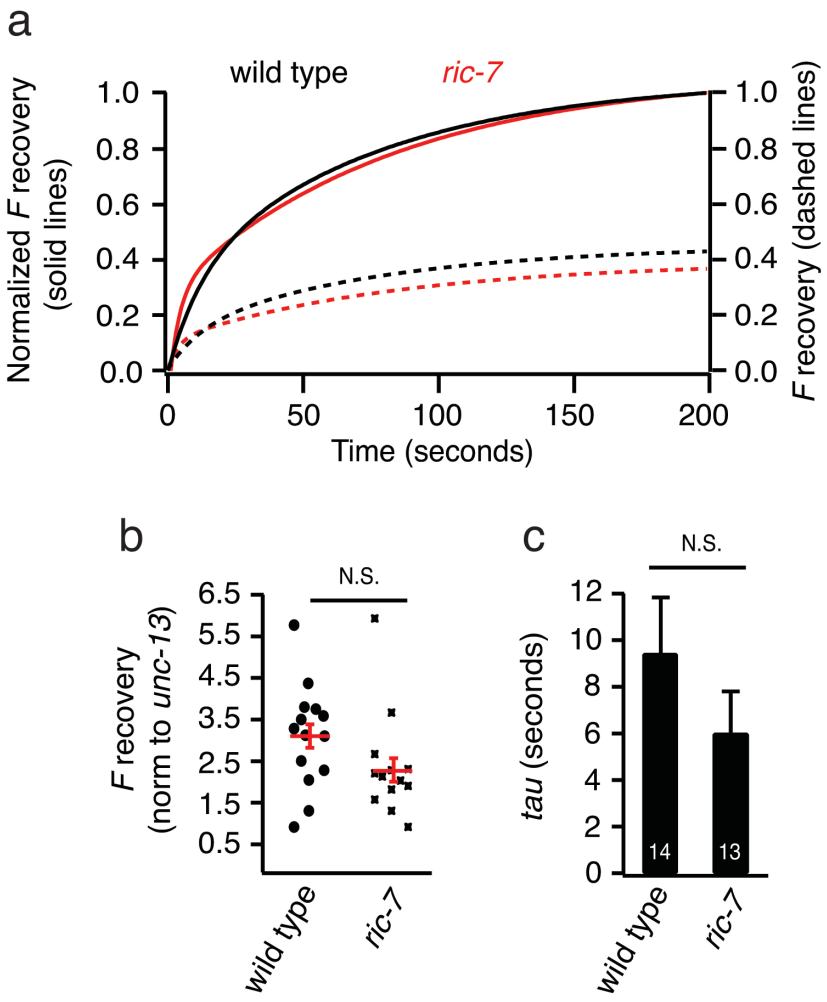


**Figure 2.11 RAB-3 exchange not altered when dense core vesicle (DCV) release is blocked.** (a) GFP::RAB-3 fitted average fluorescence recovery curves in wild type and *ric-7* mutants (dashed lines, right axis). Fitted normalized fluorescence recovery curves are also shown (solid lines, left axis). (b) Magnitude of RAB-3 fluorescence recovery (normalized to *unc-13*) at the 50 seconds time point. (c) Tau ($\tau$) values for the kinetic components of RAB-3 recovery in wild type and *ric-7* null mutants (only $\tau_{fast}$ are shown). No statistically significant differences were found (Student's t-test). The number of worms analyzed for each genotype is indicated. Error bars, standard error of the mean (SEM).

**Mutations disrupting the GTP cycle decrease RAB-3 binding to SVs**

Like all Rab proteins, RAB-3 cycles through GTP- and GDP-bound states. To investigate how the GTP cycle regulates RAB-3 function, we expressed GFP-tagged RAB-3 mutants that are locked in either the GDP- (T36N) or GTP-bound (Q81L) states (Fukuda, 2003). Neither the T36N (GDP) nor the Q81L (GTP) transgene rescued the aldicarb and EPSC defects exhibited by *rab-3* mutants (Figure 2.12), consistent with prior studies of analogous rodent Rab3 mutants (Star et al., 2005).

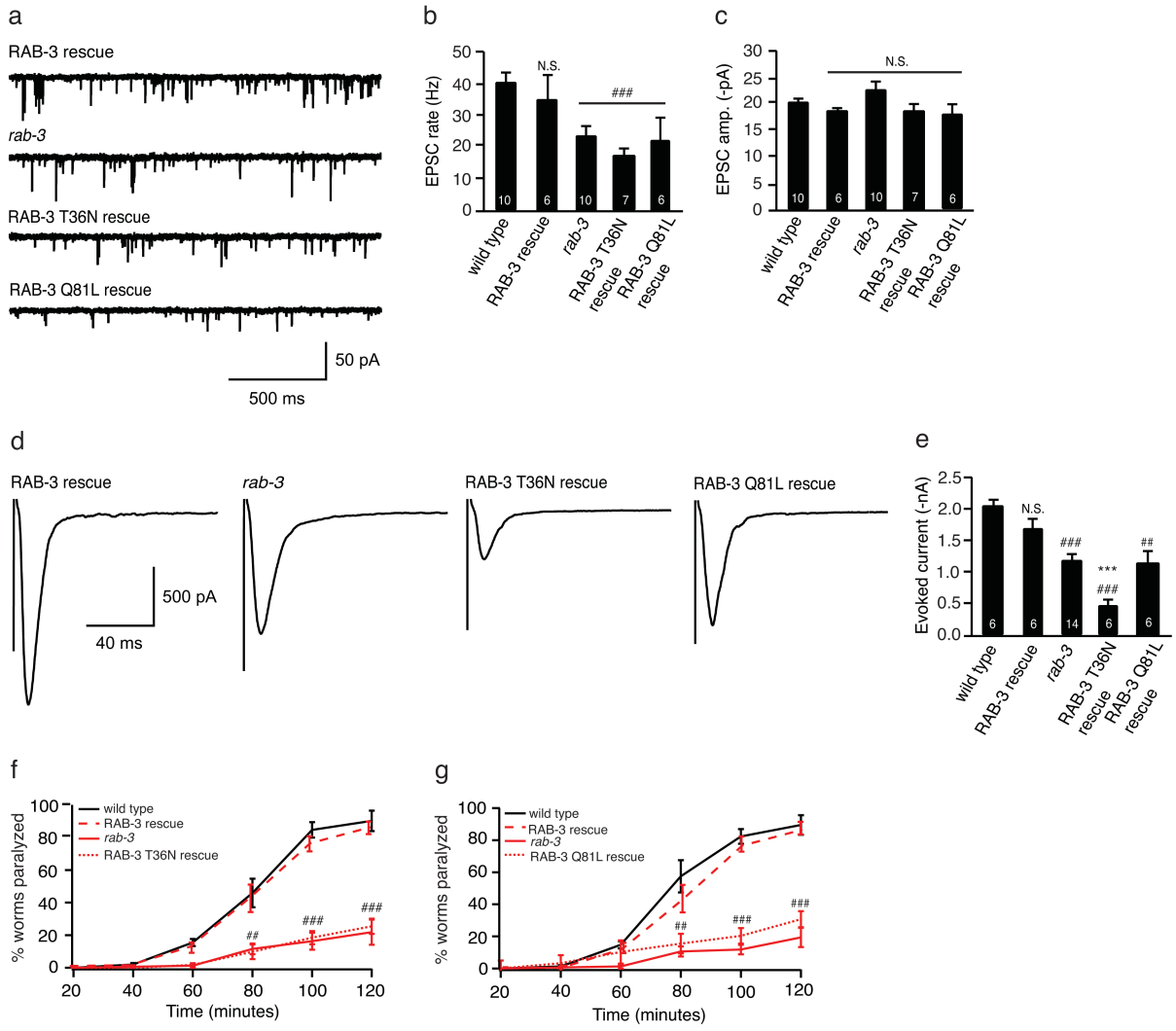


**Figure 2.12 Expression of RAB-3 T36N (GDP-locked) or RAB-3 Q81L (GTP-locked) failed to rescue the synaptic defects of *rab-3* null mutants**. (a) Spontaneous and (d) stimulus-evoked EPSCs were recorded from adult body wall muscles of the indicated genotypes. Representative traces of spontaneous EPSCs (a), averaged stimulus-evoked EPSCs (d) and summary data for both are shown (b, c and e). The number of animals analyzed is indicated for each genotype. (f-g) The paralytic response to aldicarb treatment was analyzed in the indicated genotypes (5-6 trials per genotype, ~25 animals/trial). Statistical significance noted as follows: ###, $p < 0.001$; N.S., not significant, compared to wild type; ***, $p < 0.001$, compared to *rab-3* mutants (Student's

***(Continued, Figure 2.12)*** t-test). Error bars, standard error of the mean (SEM).

As GDP-RAB-3 is extracted from membranes by GDI, we expect that T36N would be primarily cytosolic. Consistent with this idea, membrane fractionation experiments suggest that the majority of RAB-3 (T36N) is soluble (Figure 2.13a). T36N exhibited a diffuse distribution in axons with little fluorescence accumulating at synaptic puncta (puncta fluorescence = 22% total RAB-3), both indicating decreased membrane-association of RAB-3 (T36N) (Figure 2.13 b-c). A similar pattern of diffuse axonal fluorescence was observed when wild type GFP::RAB-3 was expressed in mutants lacking the AEX-3 Rab3GEF (data not shown) (Mahoney et al., 2006). Photobleaching experiments show that RAB-3 (T36N) had an enlarged mobile fraction (76%) (Figure 2.13d, right axis). When exocytosis was blocked (i.e. in *unc-13* mutants), T36N puncta fluorescence was increased (Figure 2.13 b-c) while T36N mobility was decreased (40%) (Figure 2.13d, right axis). Thus, the residual membrane-associated RAB-3 (T36N) primarily resides in the plasma membrane. Collectively these electrophysiological, biochemical and imaging observations suggest that RAB-3 (T36N) is deficient for binding to SVs, thereby disrupting its function in exocytosis.

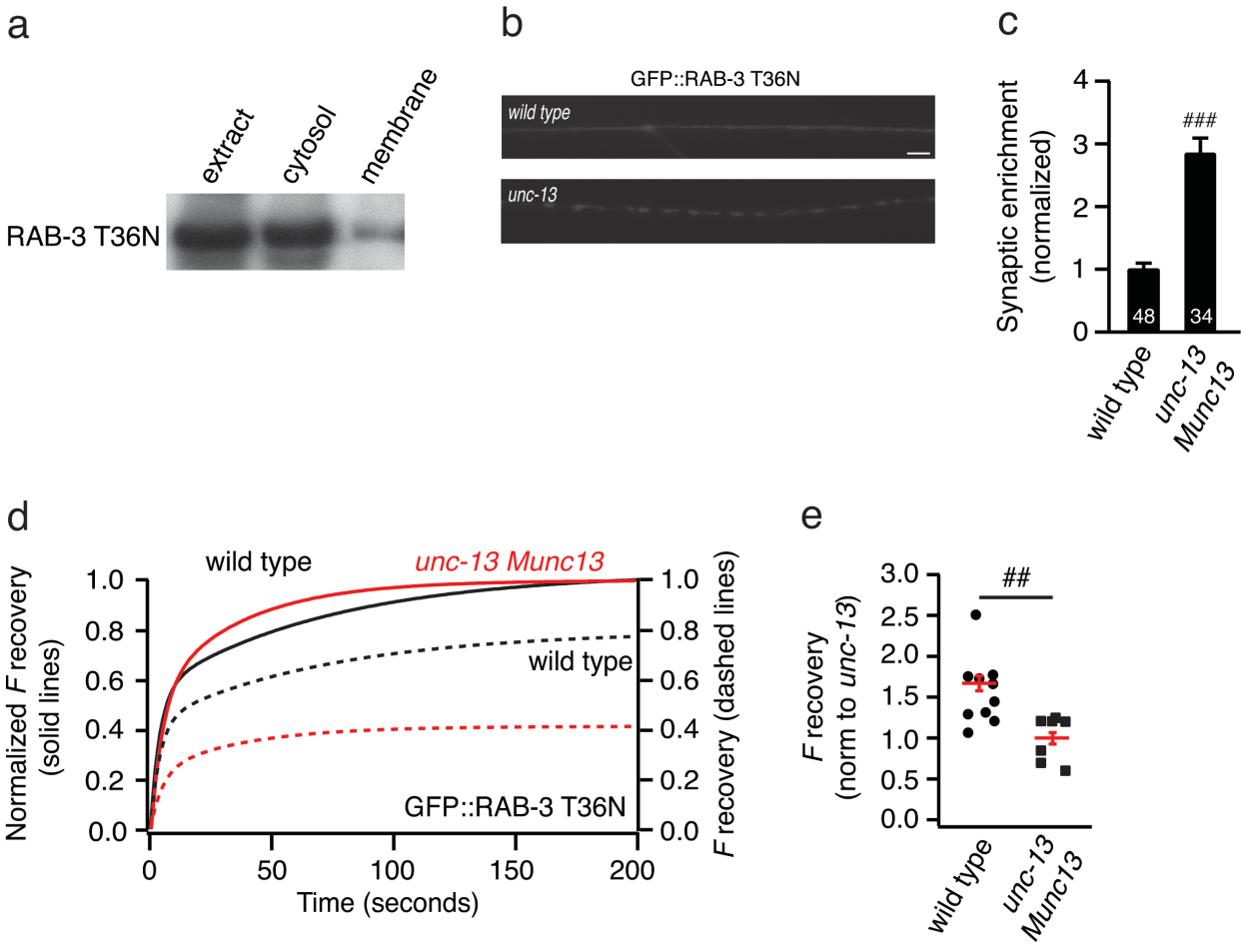


**Figure 2.13 Membrane fractionation, synaptic distribution and fluorescence recovery of GFP::RAB-3 (T36N).** (a) Western blots were performed on worm lysates from strains expressing GFP::RAB-3 (T36N) under the *unc-129* promoter. Rabbit anti-RAB-3 antibody was used. (b) Representative images and summary data (c) for GFP::RAB-3(T36N) fluorescence in the dorsal nerve cord are shown for wild type and *unc-13* mutants. Scale bar, 5 $\mu$m. (d) RAB-3(T36N) fitted average fluorescence recovery curves in wild type and *unc-13* mutants (dashed lines, right axis). Fitted normalized fluorescence recovery curves are also shown (solid lines, left axis). (e) Magnitude of RAB-3 (T36N) fluorescence recovery (normalized to *unc-13*) at the 50 seconds time point in wild type and *unc-13* mutants. Statistical significance noted as follows: ##, $p < 0.01$; ###,

***(Continued, Figure 2.13)*** $p < 0.001$, compared to wild type (Student's t-test). The number of worms analyzed for each genotype is indicated. Error bars, standard error of the mean (SEM).

Next we analyzed the behavior of GTP-locked RAB-3 (Q81L). In membrane fractionation experiments, GTP-locked RAB-3 was primarily cytosolic, (Figure 2.14a). Q81L fluorescence displayed a primarily diffuse axonal distribution (synaptic enrichment = 39%, Figure 2.14 b-c) and an increased mobile fraction (68%) (Figure 2.14d, black dashed line). In *unc-13* mutants, Q81L exhibited increased synaptic enrichment (84%, Figure 2.14 b-c) and a reduced mobile fraction (28%) (Figure 2.14d, red dashed line). In contrast, Q81L synaptic abundance (Figure 2.14 b-c) and mobile fraction (Figure 2.14e, right axis) were unaffected in *unc-10* RIM mutants, suggesting that Q81L delivery to the plasma membrane required UNC-13 but not UNC-10 (Figures 2.14 e-f). These results suggest that membrane-associated RAB-3 (Q81L) primarily resides in the plasma membrane, perhaps because it is a poor substrate for membrane extraction by GDI. Thus, both mutations blocking the GTP cycle disrupted RAB-3 function in exocytosis, most likely by preventing RAB-3 binding to SVs.

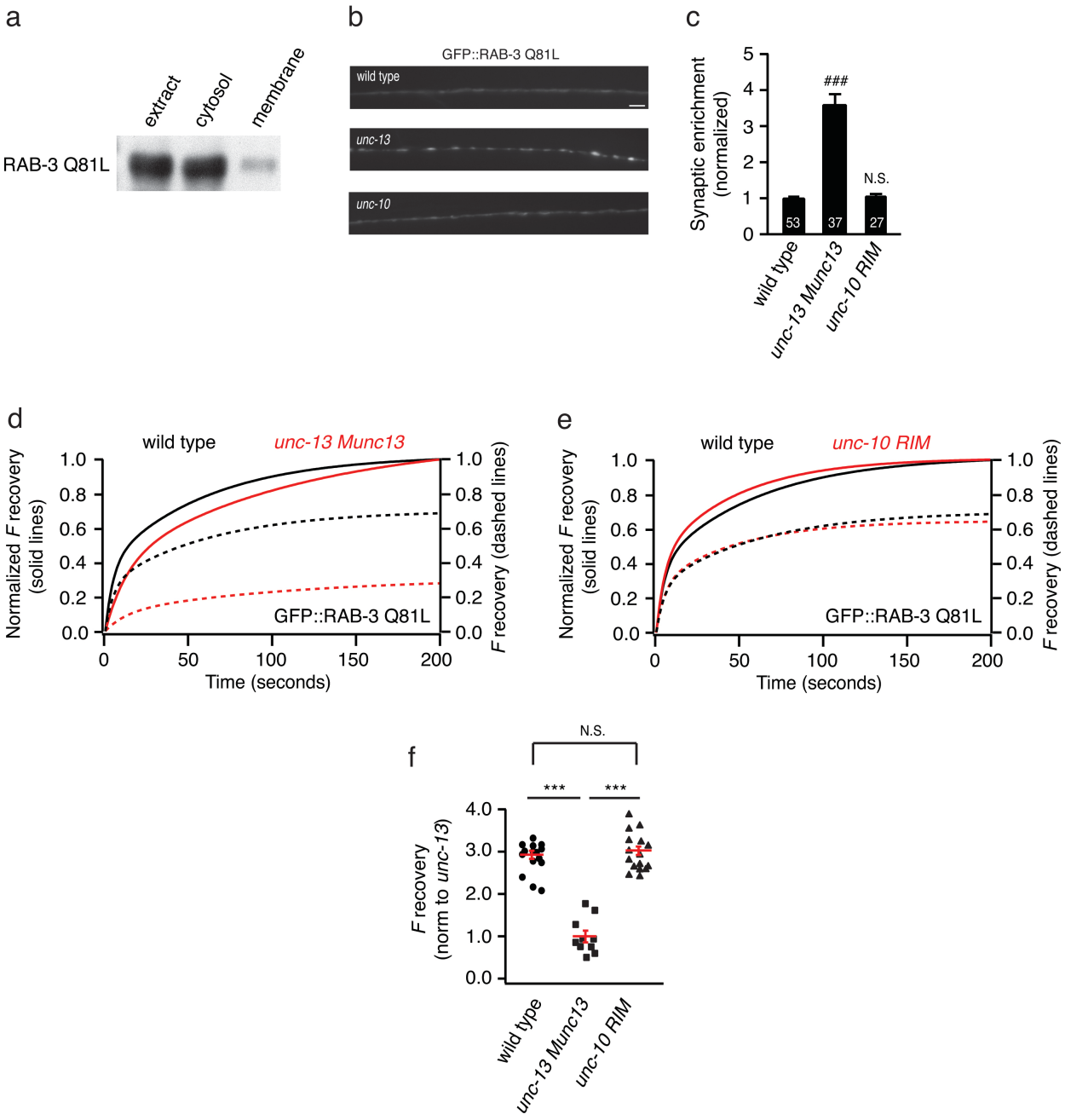


**Figure 2.14 Membrane fractionation, synaptic distribution and fluorescence recovery of GFP::RAB-3 (Q81L).** (a) Western blots were performed on worm lysates from strains expressing GFP::RAB-3 (Q81L) under the *unc-129* promoter. Rabbit anti-RAB-3 antibody was used. (b) Representative images and summary data (c) for GFP::RAB-3 (Q81L) fluorescence in the dorsal

***(Continued, Figure 2.14)*** nerve cord of wild type, *unc-13* and *unc-10* mutants. Scale bar, 5 *μ*m. (d-e) RAB-3 (Q81L) fitted average fluorescence recovery curves in wild type, *unc-13* and *unc-10* mutants (dashed lines, right axis). Fitted normalized fluorescence recovery curves are also shown (solid lines, left axis). (f) Magnitude of RAB-3 (Q81L) fluorescence recovery (normalized to *unc-13*) at the 50 seconds time point in wild type, *unc-13*, *unc-10* mutants. Statistical significance noted as follows: ###, $p < 0.001$; N.S., not significant, compared to wild type; ***, $p < 0.001$, compared to *unc-13* (Student's t-test). The number of worms analyzed for each genotype is indicated. Error bars, standard error of the mean (SEM).

We also analyzed the kinetics of RAB-3 exchange in GTP-cycle mutants. For both mutants, the fluorescence recovery was biexponential, and the rates of T36N and Q81L exchange were significantly faster than those of wild type RAB-3 (T36N: $\tau_{fast}$=2.2s, amplitude=47%, $\tau_{slow}$=43.7s, amplitude=53%; Q81L: $\tau_{fast}$=4.6s, amplitude=40%, $\tau_{slow}$=60s, amplitude=60%) (Figure 2.15 a-b, only $\tau_{fast}$ are shown). The speed of recovery of wild type RAB-3 in AEX-3 Rab3GEF mutants was similar to the observed in T36N ($\tau_{fast}$=2.9s, amplitude=45%, $\tau_{slow}$=51s, amplitude=55%) (not shown). The rate of RAB-3 exchange in GTP-cycle mutants was unaffected by mutations disrupting exocytosis (Figure 2.15 a-b). Our results suggest that GTP-cycle mutants are delivered to the plasma membrane by SV exocytosis, but they undergo exchange at an anomalous rate, most likely because of their inability to cycle between nucleotide states.

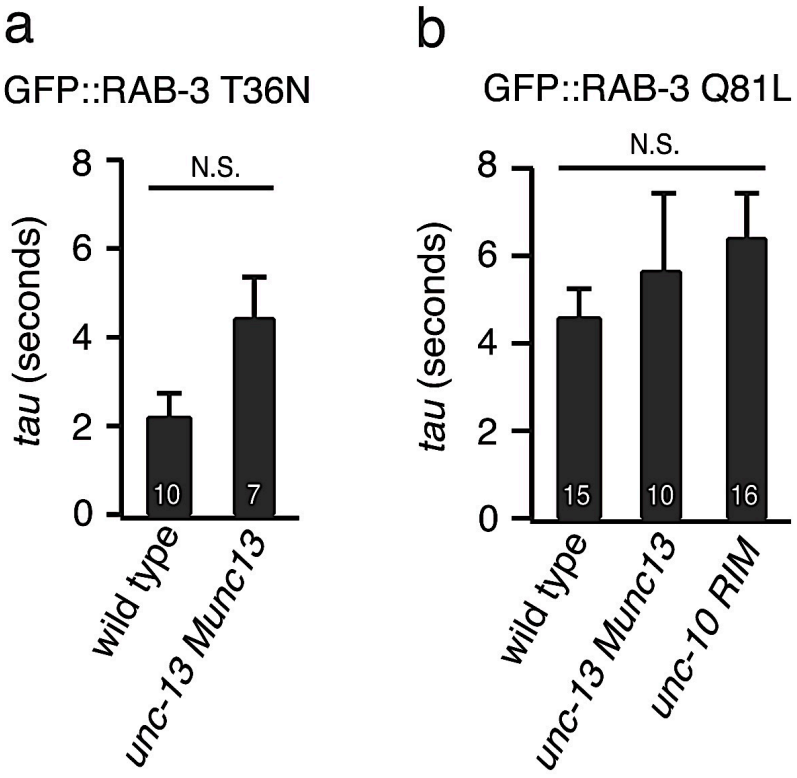


**Figure 2.15 Kinetics of recovery of RAB-3 GTP-cycle mutants.** Tau (τ) values for the kinetic components of (a) RAB-3 (T36N) and (b) RAB-3 (Q81L) fluorescence recovery in the indicated genotypes. The number of worms analyzed for each genotype is indicated. No significant differences were found. Error bars, standard error of the mean (SEM).

## DISCUSSION

Rab3 regulates several aspects of neurotransmitter release, such as synaptic vesicle (SV) fusion and release probability, and has been implicated in several forms of activity-induced synaptic plasticity (Castillo et al., 1997; Schlüter et al., 2004; Schlüter et al., 2006; Simon et al., 2008; Wang et al., 2011). To perform its role in synaptic

transmission, Rab3 must undergo a cycle of association and dissociation from SVs. Recent studies show that several presynaptic proteins, including Rab3, exhibit considerable dynamics at synapses, which are often regulated by synaptic activation (Mueller et al., 2004; Star et al., 2005; Kalla et al., 2006). Using fluorescence recovery after photobleaching (FRAP) experiments we sought to investigate how SV fusion regulates the dynamic exchange of RAB-3 at *C. elegans* neuromuscular synapses. Our results show that synaptic exocytosis regulates the dynamics of RAB-3 and that different modes of exocytosis produce distinct modes of RAB-3 mobility.

**RAB-3 dynamics depend on different exocytic proteins**

After photobleaching, synaptic RAB-3 fluorescence recovers on a timescale of tens of seconds and this recovery is mediated by RAB-3 molecules associated with the plasma membrane. Mutations decreasing SV exocytosis (i.e. *unc-13* and *unc-10*) increased the synaptic abundance of GFP-tagged RAB-3 and reduced the size of its mobile fraction, supporting the idea that RAB-3 molecules undergoing dynamic exchange at synapses are provided by SV exocytosis. Mobile RAB-3 molecules comprise two distinct pools: a rapidly exchanging pool mediated by SV exocytosis and a slower exocytosis-independent pool. The magnitude and speed of RAB-3 exchange are tightly correlated with the rate of SV exocytosis. Mutations that decrease SV exocytosis consistently decreased the rapid RAB-3 exchange but had little effect on slow exchange. Moreover, within the fast pool, RAB-3's specific exchange kinetics differed

depending on which proteins mediated an exocytosis event. Based on these results, we propose that that molecular nature of an exocytosis event determines that rate of RAB-3 dynamics in the plasma membrane. Our results also suggest that RAB-3 binding to different effectors (UNC-10 and RBF-1) may have opposite effects on RAB-3 dynamics.

**Disrupting the GTP cycle decreases RAB-3 association with SVs**

RAB-3 undergoes a cycle of association and dissociation with SVs in a manner that depends upon its bound guanine nucleotide. Prior studies suggest that the ability of Rab3 to cycle between nucleotides states is critical to its function in exocytosis (Star et al., 2005; Lin et al., 2006). Consistent with previous observations, we show that expression of GDP- (T36N) and GTP-locked (Q81L) RAB-3 is unable to rescue the synaptic defects observed in *rab-3* mutants. GTP-cycle RAB-3 mutants are largely cytosolic, most likely because they can't properly associate with membranes. A small fraction of T36N and Q81L molecules do associate with SVs and are delivered to the plasma membrane by exocytosis, where they have two kinetically distinct components. Disrupting the GTP-cycle increases the magnitude and speed of the exchanging pool of RAB-3. Blocking exocytosis reduces the magnitude of RAB-3 exchange on the plasma. In contrast to wild type RAB-3, the kinetic components of T36N and Q81L are not affected by exocytosis mutants. Altogether, our results suggest that the GTP cycle promotes RAB-3 association with SVs, which explains the synaptic defects observed in GDP- and GTP-locked mutants.

**Implications for the regulation of SV release**

Why do synapses contain two kinetically distinct pools of RAB-3? Why are kinetically distinct forms of RAB-3 exchange coupled to different exocytic events? At most synapses, neurotransmitter release is comprised by different modes of exocytosis, with distinct fusion kinetics and spatial domains, and regulated by different exocytic proteins. Our results suggest that RAB-3 associates with at least two subpopulations of SVs, regulated by the action of different exocytic proteins. Rab3 alters critical parameters of SV release and is required for certain forms of short- and long-term synaptic plasticity (Geppert et al., 1994; Castillo et al., 1997; Schlüter et al., 2004; Schlüter et al., 2006). Distinct subpopulations of SVs are specifically regulated during neuronal plasticity. Therefore, the coupling of different modes of RAB-3 mobility with different exocytosis events may contribute to the adaptive and plastic properties of neurotransmitter release. Rab3 has recently been suggested to control the composition of active zone components across release sites (Graf et al., 2009; Peled & Isacoff, 2011). It will be interesting to see if altered Rab3 dynamics are required for activity-induced changes in active zone composition.

Recent studies suggest that the availability of release sites may become limiting for synaptic transmission during repetitive stimulation (Neher & Sakaba, 2008; Neher, 2010). These studies propose that following a stimulus, exocytosis of docked and primed SVs produces an inactive release site that must be cleared before new SVs can be docked and primed. Our results provide a potential molecular mechanism to explain

release site recycling. We speculate that SV proteins (such as RAB-3) that are delivered to the plasma membrane by exocytosis must be removed from release sites through a diffusional exchange process. In this scenario, the rate of release site clearing would be correlated with the rate of RAB-3 exchange, and would differ depending on the recent activity of that synapse, and which exocytic proteins are driving release at that synapse.

## MATERIALS AND METHODS

### Strains

Strain maintenance and genetic manipulations were performed as described (Brenner, 1974). Animals were maintained at 20ºC using standard protocols, on lawns of OP50 for imaging and behavior, and on HB101 for electrophysiology. Wild type reference strain used was N2 Bristol. The following strains were used:

**Mutant strains and integrants**:

KP6221 *nuIs431* [*punc-129*::GFP::*RAB-3]*

KP6245 *unc-13(s69) I; nuIs431*

KP6261 *unc-10(md1117) X; nuIs431*

KP3292 *nuIs152 (punc129::GFP::SNB-1)*

KP3366 *unc-13(s69) I; nuIs152*

NM791 *rab-3(js49) II*

KP6262 *nuIs462 [punc-129::GFP::RAB-3 T36N]*

KP6263 *unc-13(s69) I; nuIs462*

KP6217 *nuIs430 [punc-129::GFP::RAB-3 Q81L]*

KP6264 *unc-13(s69) I; nuIs430*

KP6265 *unc-10(md1117) X; nuIs430*

KP6266 *unc-13(e1091) I; nuIs431*

KP6267 *tom-1(nu468) I; nuIs431*

KP6268 *tom1(nu468) I; unc-13(e1091) I; nuIs431*

KP6237 *aex-3(js815) X; nuIs431*

KP6269 *unc-13(e1091) I; nuIs430*

**Strains containing extrachromosomal arrays**:

KP6893 *nuEx1515 [psnb-1::UNC-13L]; unc-13(s69) I*

KP7076 *nuEx1577 [psnb-1::GFP::RAB-3]; rab-3(js49) II*

KP7077 *nuEx1578 [punc-129::ELKS-1::mCherry]; nuIs431*

KP7078 *nuEx1579 [psnb-1::GFP::RAB-3 T36N]; rab-3(js49) II*

KP7079 *nuEx1580 [psnb-1::GFP::RAB-3 Q81L]; rab-3(js49) II*

**Constructs**

Promoters utilized were *unc-129* for imaging and *snb-1* for rescue, as indicated in the text. To generate GDP-locked (T36N) and GTP-locked (Q81L) RAB-3 mutants we used site directed mutagenesis using standard PCR methods. Primers with appropriate coding mutations were generated as previously reported (Fukuda, 2003).

**Transgenes and Germline Transformation**

Transgenic strains were isolated by microinjection of various plasmids using either *pmyo-2::NLS-GFP* (KP1106) or *pmyo-2::NLS-mCherry* (KP1480) as co-injection marker at 2ng/μl. plink4 was used to balance the final DNA concentration to 100ng/μl. For imaging and rescue experiments constructs were injected at 15ng/μl. Integrated transgenes were obtained by UV irradiation of strains carrying extrachromosomal

arrays. The *nuIs152* strain has been described previously (Ch'ng et al., 2008). All integrated transgenes were out-crossed at least 6 times.

**Fluorescence Imaging**

All quantitative imaging was done using an Olympus PlanAPO 100× 1.4 NA objective and a CoolSNAP CCD camera (Hamamatsu). Worms were immobilized with 30 mg/ml BDM (Sigma). Image stacks were captured and maximum intensity projections were obtained using Metamorph 7.1 software (Molecular Devices). GFP fluorescence was normalized to the absolute mean fluorescence of 0.5 mm FluoSphere beads (Molecular Probes). Young adult worms, in which the dorsal cords were oriented toward the objective, were imaged in the region just posterior to the vulva. Line scans of dorsal cord fluorescence were analyzed in Igor Pro (WaveMetrics) using custom-written software (Dittman & Kaplan, 2006). Briefly, “peak” is the ratio of peak fluorescence to the fluorescent slide standard. “Axon” is the ratio of baseline fluorescence (the minimum fluorescence level over a 5 µm interval within the dorsal cord image) to the fluorescent slide standard. “Synaptic Enrichment” (% $\Delta F/F$) is defined as $(F_{peak} - F_{axon})/F_{axon}$. All the values reported in the figures are means ± standard error of the mean (SEM). Statistical significance was determined using a two-tailed Student's t test.

**Photobleaching**

To image GFP we used 0.5% power from a 473 nm Argon laser. Five frames of GFP signals were recorded prior to photobleaching. Photobleaching was achieved by one scan (90% power from a 473 nm Argon laser) on a rectangular region of interest (ROI, about 2 × 1.5 μm) that covers a single GFP punctum. GFP signals were further recorded for 200 seconds with a rate of 0.5 frames/second. To avoid artifacts caused by animal movement or sample drifting, traces with more than 10% decrease in GFP signals were discarded. Fluorescence dispersion time constants (*tau*, $\tau$) were obtained by fitting the data with a single or a double exponential function, as indicated in the text. To isolate the exocytosis-dependent of RAB-3 fluorescence recovery we subtracted the average RAB-3 recovery observed in *unc-13* null mutants (Figure 2.7, red line) from the average RAB-3 recovery in wild type animals (Figure 2.7, black line). The results of this subtraction (Figure 2.7, grey line) were used to determine the time point at which most of the exocytosis-dependent (i.e. UNC-13) recovery of RAB-3 (50 seconds, Figure 2.7 indicated by black dashed line) had occurred. Statistical significance was determined using Student's t test and all values reported are means ± SEM.

**Membrane Fractionation**

Subcellular fractionation was performed on a mixed population of worms expressing *unc-129* driven GFP::RAB-3 (wild type, T36N or Q81L). Membrane extracts were isolated as previously described (Dreier et al., 2005). The fraction of membrane-

associated and cytosolic GFP::RAB-3 was determined by Western blotting of membrane and cytosol fractions with a rabbit anti-RAB-3 antibody (gift from Michael Nonet).

**Aldicarb assays**

Aldicarb assays were performed on young adult worms as described (Lackner et al., 1999). Briefly, worms were exposed to 1.5 mM aldicarb for 2 hours, with paralysis being assessed every 20 minutes. Each assay was repeated 5-6 times, with ~25 animals per trial.

**Electrophysiology**

Strains for electrophysiology were maintained at 20°C on plates seeded with HB101. Adult worms were immobilized on Sylgard-coated coverslips with cyanoacrylate glue. Dissections and whole-cell recordings were carried out as previously described ( Richmond & Jorgensen, 1999; Madison et al., 2005). Statistical significance was determined using the Student's t-test for comparison of mean frequency and amplitude for endogenous EPSCs.

# CHAPTER 3

# REGULATION OF RAB-3 BY A G-PROTEIN COUPLED PATHWAY

Monica Ivelisse Feliu-Mojer performed all the experiments described in this chapter.

## INTRODUCTION

As discussed in Chapters 1 and 2 of this Dissertation, the regulation of the small GTPase RAB-3 could provide a biochemical mechanism for altering synaptic vesicle (SV) release. One such mechanism could be the modulation of synaptic strength by G-protein coupled receptors (Lackner et al., 1999).

In *C. elegans*, G-protein coupled signaling pathways extensively regulate neurotransmission, including antagonistic regulation of ACh secretion by $G\alpha_o$ (GOA-1) and $G\alpha_q$ (EGL-30). In motor neurons, EGL-30 $G\alpha_q$ has been shown to mediate facilitation of cholinergic synaptic transmission (Lackner et al., 1999). In vertebrates, $G\alpha_q$ activates phospholipase C beta (PLCβ) isoforms, which hydrolyze phophatidylinositol bisphosphate ($PIP_2$) to inositol 1,4,5-triphosphate ($IP_3$) and diacylglycerol (DAG). $IP_3$ and DAG then go on to act on several targets. A well-conserved variation of this pathway appears to be employed in *C. elegans* motor neurons to modulate ACh release (Bastiani & Mendel, 2006). Activation of EGL-30 leads to the activation of EGL-8 PLCβ, causing an increase in the concentration of DAG. Presynaptic DAG recruits UNC-13 Munc13, a protein required for synaptic vesicle priming (Lackner et al., 1999). Treatment with phorbol esters (a synthetic DAG agonist) restores normal ACh release to *egl-30* or *egl-8* mutants, and this effect is mediated in part by the presynaptic DAG-binding protein UNC-13 (particularly its short isoform, UNC-13S) (Lackner et al., 1999). Thus, presynaptic EGL-30 acts to promote synaptic vesicle release in cholinergic synapses.

Evidence suggests a link between EGL-30 and RAB-3 in presynaptic function. An RNAi screen done in our lab to identify DAG/phorbol esters targets showed that inactivation of RAB-3 (by RNAi and null mutations) confers resistance to phorbol esters (Sieburth et al., 2005). Another report from our lab showed that animals with reduced EGL-30 activity display a significant decrease in RAB-3 punctal fluorescence (Ch'ng et al., 2008). Together, these results suggest that RAB-3 activity may be regulated by EGL-30 and DAG. The EGL-30 pathway has been previously shown to modulate ACh release in worms and the small GTPase RAB-3 also regulates SV vesicle fusion at the *C. elegans* neuromuscular junction (NMJ) (Nonet et al., 1997). Thus, regulation of RAB-3 by EGL-30 could provide another mechanism to modulate presynaptic ACh release at the *C. elegans* NMJ.

Recently, our lab has shown that the cholecystokinin (CCK)-gastrin-like neuropeptide NLP-12 mediates a pathway that potentiates ACh release via a putative a $G\alpha_q$/PLCβ pathway (Janssen et al., 2008; Hu et al., 2011). In *C. elegans*, NLP-12 is secreted from a single neuron (e.g. DVA) in response to muscle contraction. Activation of the receptor CKR-2 by NLP-12 potentiates synaptic transmission at cholinergic NMJs (Hu et al., 2011).

In this chapter we use the activation of the NLP-12 pathway as a model to test the regulation of RAB-3 by a $G\alpha_q$-coupled pathway. First, we acutely evoked NLP-12 secretion in wild type, *nlp-12*, *ckr-2*, *egl-30* and *egl-8* mutants expressing YFP::RAB-3 in

the dorsal nerve cord (DNC). Then, we performed imaging experiments to test if and how the NLP-12 pathway regulates RAB-3.

## RESULTS

NLP-12 is a cholecystokinin (CCK)-gastrin-like neuropeptide released by the single tail neuron DVA in *C. elegans* in response to muscle contraction (Hu et al., 2011). To evoke NLP-12 secretion, we treated worms with the cholinesterase inhibitor aldicarb. A brief treatment with aldicarb causes an accumulation of ACh at NMJs, inducing body wall muscle contraction. To determine the effects of aldicarb-induced acute NLP-12 secretion on RAB-3, we treated worms expressing YFP::RAB-3 in DA and DB neurons (under the *unc-129* promoter) with aldicarb for 1 hour, and then proceeded to image them. We found that aldicarb treatment resulted in a significant increase in RAB-3 synaptic enrichment in the dorsal axons of wild type animals (Figure 3.1).

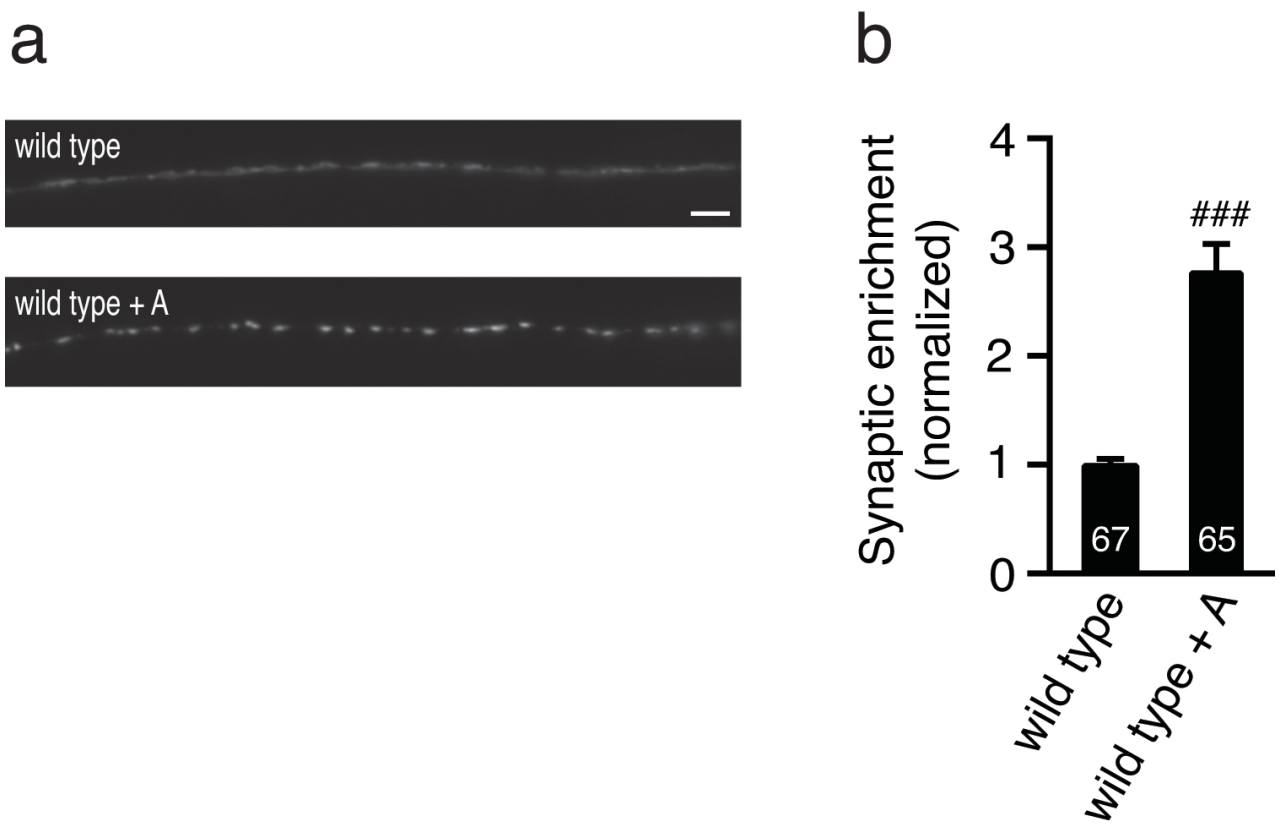


**Figure 3.1 Aldicarb induces a significant increase in RAB-3 synaptic enrichment.** (a) Representative images and (b) summary data for YFP::RAB-3 fluorescence in the dorsal nerve cord are shown for wild type animals, with and without aldicarb treatment. The number of worms analyzed for each genotype and treatment is indicated. Statistical significance noted as follows: ###, $p < 0.001$, compared to untreated wild type controls (Student's t-test). Scale bar, 5 $\mu$m. Error bars, standard error of the mean (SEM).

If the aldicarb-induced increase in RAB-3 synaptic fluorescence we observe is due to NLP-12 secretion and subsequent CKR-2 activation, then *nlp-12* and *ckr-2* mutations should suppress this effect. RAB-3 fluorescence was significantly increased

in *nlp-12* and *ckr-2* mutants after a 1-hour aldicarb treatment. Thus, *nlp-12* and *ckr-2* mutations do not suppress the effect of aldicarb on RAB-3 fluorescence (Figure 3.2).

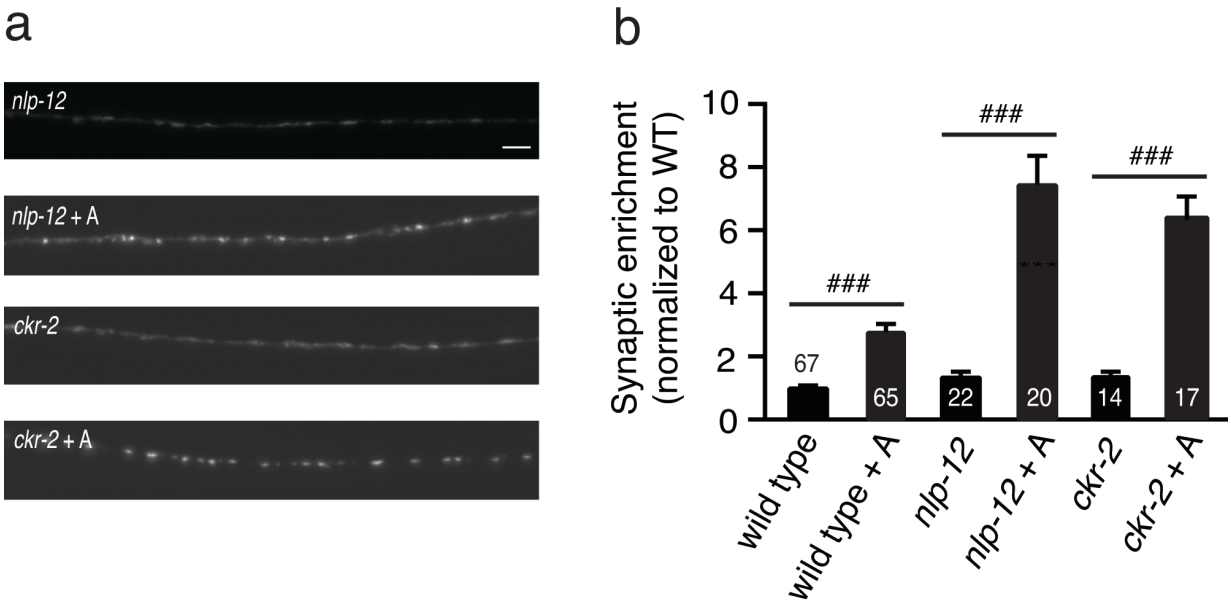


**Figure 3.2 *nlp-12* and *ckr-2* mutations do not suppress the aldicarb-induced synaptic enrichment of RAB-3.** (a) Representative images and (b) summary data for YFP::RAB-3 fluorescence in the dorsal nerve cord are shown for wild type, *nlp-12* and *ckr-2* mutants, with and without aldicarb treatment. The number of worms analyzed for each genotype and treatment is indicated. Statistical significance noted as follows: ###, $p < 0.001$, compared to untreated control (Student's t-test). Scale bar, 5 $\mu$m. Error bars, standard error of the mean (SEM).

Mutations to *egl-30* and *egl-8* also failed to suppress the aldicarb-induced increase in RAB-3 synaptic enrichment (Figure 3.3). Collectively, our results suggest that the significant increase in RAB-3 synaptic enrichment we observe in dorsal synapses of wild type animals is not mediated by the $G\alpha_q$-coupled NLP-12 pathway.

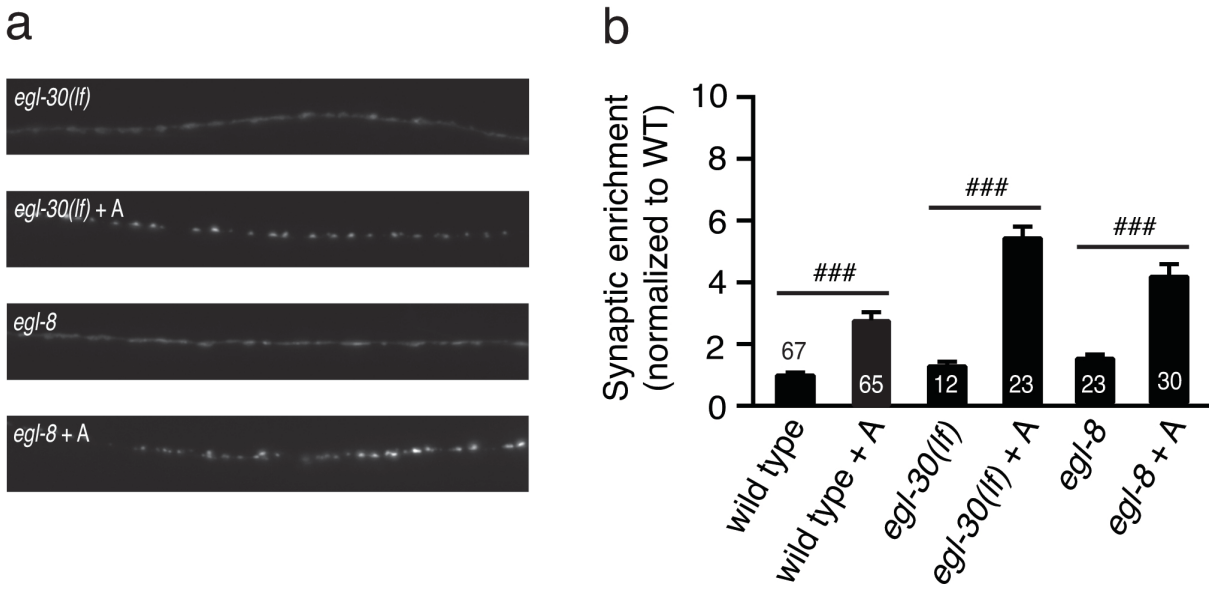


**Figure 3.3 *egl-30(lf)* and *egl-8* mutations do not suppress the aldicarb-induced synaptic enrichment of RAB-3.** (a) Representative images and (b) summary data for YFP::RAB-3 fluorescence in the dorsal nerve cord are shown for wild type, *egl-30* loss of function and *egl-8* mutants, with and without aldicarb treatment. The number of worms analyzed for each genotype and treatment is indicated. Statistical significance noted as follows: ###, $p < 0.001$, compared to untreated control (Student's t-test). Error bars, standard error of the mean (SEM). Scale bar, 5 $\mu$m.

## DISCUSSION

The EGL-30 $G\alpha_q$-coupled pathway has been shown to mediate facilitation of cholinergic synaptic transmission at the *C. elegans* NMJ (Lackner et al., 1999). Recent evidence suggests that RAB-3 may be a target of the EGL-30 pathway that regulates cholinergic release (Sieburth et al., 2005; Ch'ng et al., 2008). To characterize how the $G\alpha_q$/PLCβ pathway regulates RAB-3, we sought to use the activation (via aldicarb treatment) of a recently identified endogenous neuropeptide (NLP-12) pathway that potentiates ACh release via the $G\alpha_q$/PLCβ signaling cascade (Hu et al., 2011).

Our experiments show that aldicarb treatment induces an increase in the synaptic enrichment of RAB-3 fluorescence in the dorsal nerve cord axons of wild type worms. Our current results argue against the hypothesis that this effect is mediated by secretion of NLP-12 and subsequent activation of a $G\alpha_q$/PLCβ via its CKR-2 receptor. Mutations to *nlp-12*, *ckr-2*, *egl-30* and *egl-8* all failed to suppress the aldicarb-induced increase in RAB-3 synaptic enrichment.

All the RAB-3 imaging reported here was done in dorsal synapses. RAB-3 expression was driven by the *unc-129* promoter, which controls expression in a subset of cholinergic neurons (i.e. DA and DB neurons) that innervate dorsal body wall muscles (Goodwin et al., 2012). NLP-12 is expressed in a single tail neuron, DVA, which has one axon that runs along the animal on its ventral side (Janssen et al., 2008; Hu et al., 2011). Therefore, anatomically, the source of NLP-12 secretion is far from the dorsal cholinergic synapses being imaged here. CKR-2 receptors are expressed in all

cholinergic neurons, including DA and DB (Hu et al., 2011). Thus we consider it unlikely that a lack of CKR-2-receptor expression in DA and DB neurons can explain our negative results. NLP-12 behaves differently from other previously analyzed fluorescently-tagged neuropeptides and appears to be unable to diffuse far from the ventral cord tissue (Hu et al., 2011). Only DVA expression of NLP-12 is able to rescue the synaptic transmission defects and the suppression of aldicarb-induced potentiation observed in *nlp-12* mutants. Thus, NLP-12 seems to have a ventral, but not a dorsal site of action, raising the possibility that, in our experiments, aldicarb exposure induced NLP-12 release, but that the released NLP-12 was physically unable to reach the target imaging area (dorsal synapses). Imaging of RAB-3 expressed in the ventral nerve cord following aldicarb treatment would be necessary to test this hypothesis. Certainly further experiments are needed to elucidate the downstream effectors of the NLP-12/CKR-2 pathway, how it acts to potentiate cholinergic release, and how RAB-3 may be involved in this or other EGL-30/EGL-8-coupled pathways.

Although not mediated by NLP-12, we did observe an aldicarb-induced increase in RAB-3 synaptic enrichment. It is possible that this effect is regulated by the activation of a different neuropeptide-mediated pathway. One way to address this question would be to test if mutations to the genes encoding the proneuropeptide-processing proteins EGL-3 and EGL-21 are able to suppress the increase in RAB-3 accumulation induced by aldicarb exposure. If the aldicarb-induced accumulation of RAB-3 is suppressed by *egl-3* or *egl-21* mutations, one could do an RNAi screen to test if knockdown of one or

several of the 115 proneuropeptide genes in the *C. elegans* genome can suppress the aldicarb-induced accumulation of RAB-3 (Li et al., 2006).

Our lab has previously shown that brief aldicarb treatments produce a form of activity-induced synaptic potentiation. We observe that such aldicarb treatments induced an increase in synaptic RAB-3 accumulation in dorsal synapses. Although the mechanisms for this increase remain unknown, we believe that our experiments would provide a framework for further investigation of the role of RAB-3 in synaptic potentiation at the *C. elegans* NMJ.

## MATERIALS AND METHODS

### Strains

Strains were maintained at 20ºC using standard protocols, on lawns of OP50 for imaging. The following strains were used:

KP3931 *nuIs168* [*punc-129*::YFP::*RAB-3*]

KP6259 *nlp-12(ok335)*; *nuIs168*

KP6260 *ckr-2(tm3082)*; *nuIs168*

KP4168 *egl-30(ad806)*; *nuIs168*

KP4166 *nuIs168*; *egl-8(sa47)*

### Aldicarb treatment and fluorescence imaging

All quantitative imaging was done as previously described (Chapter 2). Imaging was done in either untreated animals or animals exposed to 1.5 mM aldicarb for 60 minutes (Hu et al., 2011). For all comparisons of control and aldicarb treated animals of the same genotype, statistical significance was determined using a two-tailed Student's t-test.

# CHAPTER 4

# DISCUSSION AND FUTURE DIRECTIONS

**Regulation of RAB-3 dynamics by exocytosis**

In order to maintain adequate synaptic transmission, neurons must tightly regulate the series of steps that lead to SV release, such as docking of vesicles at release sites, priming, and calcium-evoked exocytosis. These steps are orchestrated by several evolutionarily conserved proteins, which ensure the temporal and spatial regulation of release. Thus, understanding the dynamics of the molecular components that govern SV exocytosis will provide insights into the presynaptic mechanisms that regulate synaptic transmission. In this Dissertation, we analyzed the dynamic exchange of the small GTPase RAB-3 at *C. elegans* neuromuscular synapses. We show that synaptic exocytosis regulates the dynamics of RAB-3. We also show that RAB-3's exchange kinetics in the plasma membrane differ depending on which proteins mediated an exocytosis event. We propose that the coupling of different modes of RAB-3 mobility with different exocytosis events may contribute to the adaptive and plastic properties of neurotransmitter release. By being coupled to different exocytosis events RAB-3 could be a substrate to regulate different modalities of synaptic transmission.

**Dynamics of active zone composition**

Rab3 has recently been implicated in controlling the composition of active zone components across release sites (Graf et al., 2009; Peled & Isacoff, 2011). At the Drosophila NMJ, Rab3 regulates the dynamic distribution of the presynaptic protein

Bruchpilot (Brp, an ortholog of CAST/ELKS) and calcium channels (Graf et al., 2009). CAST/ELKS proteins interact with several active zone proteins, including the Rab3 effector RIM; however, RIM does not appear to function in the Rab3-mediated regulation of Brp distribution (Graf et al., 2012). In *C. elegans* the Bruchpilot homolog ELKS-1 cooperates with SYD-2/$\alpha$-liprin in the assembly of presynaptic active zone formation (Dai et al., 2006). Although it appears to be important for the molecular organization of presynaptic release, the exact function of ELKS remains enigmatic. Based on these previous reports, it would be interesting to further investigate ELKS-1 and how it may be regulated by RAB-3 using FRAP as described in Chapter 2. We show that many RAB-3 puncta colocalize with ELKS-1 puncta (Figure 2.4). To investigate whether RAB-3 regulates the distribution of ELKS-1 in *C. elegans*, one could test whether the synaptic distribution and dynamics of fluorescently-tagged ELKS-1 is altered in *rab-3* mutants. The dynamics of RAB-3 exchange are different depending on which exocytic proteins are driving release at that synapse. One could test how different exocytic events affect the dynamics of ELKS-1 by doing FRAP experiments in mutants (i.e. *unc-13* mutants, *unc-10*, *rbf-1*) expressing GFP-tagged ELKS-1.

Recent studies have suggested that the availability of release sites may become limiting for synaptic transmission during repetitive stimulation (Neher, 2010; Neher & Sakaba, 2008). These studies propose that following a stimulus, exocytosis of docked and primed SVs produces an inactive release site that must be cleared before new SVs can be docked and primed at that site. In Chapter 2 we propose that vesicular proteins

such as RAB-3 are delivered to the plasma membrane by exocytosis and must be removed from release sites by a diffusional exchange process. Our results indicate that the speed of this exchange process depends on the molecular identity of the fusion event. Thus, it would be interesting to use photobleaching experiments to analyze the dynamics of other vesicular and/or active zone proteins and study the pathways that regulate their exchange after being deposited in the plasma membrane by exocytosis. Recently, studies using FRAP have indicated that several presynaptic components exhibit considerable dynamics, which are often accelerated by synaptic activation (Mueller et al., 2004; Star et al., 2005; Kalla et al., 2006). Our lab has strains expressing GFP-tagged versions of several presynaptic proteins (i.e. SNB-1 synaptobrevin, SNN-1 synapsin) (Sieburth et al., 2005; Ch'ng et al., 2008) which would allow us to do FRAP experiments and ask how the mobility of these presynaptic proteins changes in response to synaptic activity.

In Chapter 2 we show that UNC-13L, UNC-13S and TOM-1 differentially affect the exchange of synaptic RAB-3. Recent results from our lab indicate that UNC-13L, UNC-13S and TOM-1 form a molecular code that dictates the timing of neurotransmitter release (Hu et al., unpublished). These results suggest that fast and slow release comprise independent exocytosis mechanisms that operate in parallel and thus can be adjusted independently to modulate neurotransmitter release. Rab3 regulates critical presynaptic parameters (i.e. the number of docked vesicles and the probability of SV fusion) and consequently modulates synaptic transmission (Geppert et al., 1994;

Castillo et al., 1997; Nonet et al., 1997; Schlüter et al., 2004; Schlüter et al., 2006). Thus, it is interesting to speculate that RAB-3 may also be involved in regulating the timing of neurotransmitter release.

**Coupling the Rab3 cycle to different modes of SV exocytosis**

In parallel to the SV cycle, Rab3 undergoes a cycle of association with donor (i.e. SV) and dissociation from target membranes (i.e. presynaptic plasma membrane) (von Mollard et al., 1991) via a GTP-dependent mechanism. Our results suggest that the GTP cycle promotes RAB-3 association with SVs and that RAB-3 must be able to cycle between nucleotide states to properly regulate SV exocytosis. Several aspects of the Rab3 cycle remain poorly understood. How is SV exocytosis coupled to changes in Rab3 activity? What is the relationship between nucleotide exchange and the rate of exchange on the plasma membrane? How is nucleotide exchange coupled to different exocytic events? To address this, FRAP experiments could be performed in *unc-13* null, *unc-13(e1091)*, *unc-13s*, *tom-1*, *unc-10*, and *rbf-1* mutants expressing GFP-tagged RAB-3(T36N) and RAB-3(Q81L) to test how RAB-3 exchange is affected in these mutants. One could plot the magnitude and rate of exchange of these GTP-cycle mutants versus the rate of exocytosis in these 6 genotypes (and wild type) to see if their relationship to mEPSC rate is distinct from WT RAB-3. Active Rab3 is GTP-liganded and primarily associated with SVs (von Mollard et al., 1990). Similarly, Rab3 only binds to its effectors in its GTP-bound states. To further investigate RAB-3 activity, one could

use a mCherry-tagged version of the Rab binding domain of the Rab3 effector RIM (RBD/mCherry) available in the lab. The RIM RBD domain binds selectively to RAB-3-GTP; consequently, this fluorescent protein would provide an optical assay for the distribution of "active" RAB-3-GTP and how that distribution is affected by synaptic activity.

**Regulators of the RAB-3 cycle**

The guanine nucleotide-binding status of Rabs is modulated by several regulatory proteins (i.e. GDI, Rab3GEF and Rab3GAP). In theory, any step of the Rab3 cycle could be regulated at the synapse to alter Rab3 activity and in turn affect synaptic vesicle release. Little is known about how Rab regulatory proteins affect SV release, but given Rab3's role in the regulation of SV exocytosis, it seems logical that regulators of Rab3 will also modulate synaptic transmission. For example, AEX-3 Rab3GEF catalyzes the GDP-GTP exchange that activates RAB-3. RAB-3 association with SV requires normal AEX-3 Rab3GEF function (Iwasaki et al., 1997; Mahoney et al., 2006). We show that the dynamics of RAB-3 in *aex-3 Rab3GEF* mutants are very similar to the dynamics of GDP-locked RAB-3, consistent with the idea that AEX-3 promotes RAB-3 association with SVs. Very little is known about the synaptic distribution and dynamics of Rab3GEF, information that could provide insights into how AEX-3 regulates RAB-3 activity and its association with SVs. One could use FRAP experiments to assess these parameters and how they may be affected in exocytic mutants. During my time in the

lab, I constructed a plasmid to express GFP-tagged AEX-3 under the *snb-1* promoter, which was able to rescue the aldicarb-resistant phenotype of *aex-3* mutants indicating that it is functional. An *unc-129* driven GFP-tagged AEX-3 could be constructed to do the aforementioned FRAP experiments. At some point during or after fusion GTP hydrolysis is catalyzed by Rab3GAP, making GDP-RAB-3 available for removal from the plasma membrane by GDI. Currently the mechanisms that recruit or trigger Rab3GAP activity are unknown. Unfortunately, the identity of the *C. elegans* homolog for Rab3GAP homolog is also unknown. Recently RBG-1 has been identified as a potential Rab3GAP homolog, but its function is yet to be characterized. The characterization of RBG-1 as a Rab3GAP or the identification of a novel protein with Rab3GAP activity remains an important step towards understanding how the RAB-3 cycle is coupled to SV exocytosis.

**A framework to study the role of RAB-3 in synaptic plasticity**

Our lab has previously shown that brief treatments with the acetylcholine esterase inhibitor aldicarb induces a form of synaptic potentiation, which is abolished in neuropeptide deficient mutants (Hu et al., 2011). In Chapter 3, we show that brief aldicarb treatments induce an increase in the synaptic enrichment of RAB-3 fluorescence in the dorsal nerve cord axons of wild type worms. These observations could provide a framework to study the role of RAB-3 in activity-dependent synaptic potentiation and more generally, in synaptic plasticity. How does aldicarb treatment

induce synaptic accumulation of RAB-3? Because our lab has already established the identity of the signal (i.e. NLP-12) and the receptor (i.e. CKR-2) that mediate aldicarb-induced synaptic potentiation in ventral synapses, it would be best to image ventrally expressed GFP-tagged RAB-3 to address this question. Presuming that a brief treatment with aldicarb would induce an increase in RAB-3 accumulation in ventral synapses, one could then investigate whether this effect is mediated by the NLP-12 pathway by testing if mutations to *nlp-12*, *ckr-2*, *egl-30* and *egl-8* can block this increase. One could do the corresponding electrophysiology experiments to test whether mutations to *rab-3*, *egl-30* and *egl-8* can block aldicarb-induced synaptic potentiation (recordings are commonly done on ventral, but not dorsal body muscles). This paradigm for activity-induced synaptic potentiation can also be used to investigate how RAB-3 dynamics may be altered during synaptic plasticity. Are the magnitude and rate of RAB-3 exchange altered after aldicarb treatment? Because RAB-3 synaptic enrichment is increased after aldicarb treatment, one would expect so. FRAP experiments similar to the ones described in Chapter 2 could be performed to further explore this idea.

Rab3 regulates two critical presynaptic parameters – the number of docked vesicles at synapses, and the probability of vesicle release after depolarization. At least three types of activity-induced synaptic plasticity involve the action of Rab3. In vertebrates, Rab3 is essential for mossy fiber long-term potentiation (Castillo et al., 1997; Lonart et al., 1998) and has been proposed to act on a subset of SVs (Schlüter et

al., 2006) to regulate short-term synaptic plasticity. At vertebrate and invertebrate NMJs, Rab3 is involved in mechanisms of homeostatic plasticity. Lack of Rab3 function impairs the activity-induced homeostatic increase in quantal response amplitude at the mouse NMJ (Wang et al., 2011). In *Drosophila*, Rab3, its Rab3GAP and its effector RIM have been suggested to participate in a presynaptic signaling system that controls the expression of synaptic homeostasis (Muller et al., 2011; Muller et al., 2012). Finally, previous work from our lab identified RAB-3 as a downstream target for the regulation of neurotransmitter release by retrograde synaptic signals (Simon et al., 2008). Consequently, a detailed of understanding of the mechanisms that regulate RAB-3 will shed light on how the regulation of RAB-3 could provide a biochemical mechanism for modifying synaptic transmission.

**Concluding remarks**

The results and observations presented in this Dissertation provide a framework to further explore the dynamics of RAB-3 at synapses as well as the role of RAB-3 in the regulation of synaptic transmission and plasticity. Moreover, the experiments discussed in this Dissertation could be used to further investigate the role of a second small GTPase (i.e. AEX-6 Rab27) in SV exocytosis. Rab27 is the Rab protein most closely related to Rab3 and like Rab3 it associates with SVs and promotes SV fusion (Fukuda et al., 2004; Mahoney, 2006). In *C. elegans*, *rab-3* and *aex-6* Rab27 double mutants have more severe synaptic transmission defects than single mutants, implying that

RAB-3 and AEX-6 Rab27 act in parallel pathways to regulate synaptic transmission. Very little is known about how RAB-27 is regulated.

We hope that the work presented in this Dissertation and future studies provide insights not only about the role of Rab3 in the regulation of neurotransmitter release, but also valuable insights for Rab proteins generally.

# APPENDIX 1

## ADDITIONAL ANALYSIS OF RAB-3 FLUORESCENCE RECOVERY

Monica Ivelisse Feliu-Mojer performed all the experiments described in this appendix.

## OVERVIEW

In addition to the genotypes we described in Chapter 2, we analyzed the exchange kinetics of RAB-3 in worms lacking both RAB-3 putative effectors, UNC-10 RIM and RBF-1 Rabphilin.

## RATIONALE

The results detailed in Chapter 2 suggest that RAB-3 binding to different effectors may have opposite effects on RAB-3 dynamics (i.e. RBF-1 may act to accelerate RAB-3 exchange while UNC-10 slows it down) (Figure 2.9). This prompted us to analyze RAB-3 mobility in *unc-10; rbf-1* mutants, which lack both putative effectors of RAB-3.

## RESULTS

In contrast to *unc-10* single mutants, the magnitude of RAB-3 recovery in *unc-10; rbf-1* double mutants is similar to wild type controls (and *rbf-1* mutants) (Figure A.1b). The kinetics of recovery of RAB-3 in *unc-10; rbf-1* double mutants are single exponential and slower than wild type, but not significantly different from *unc-10* or *rbf-1* (Figure A.1c).

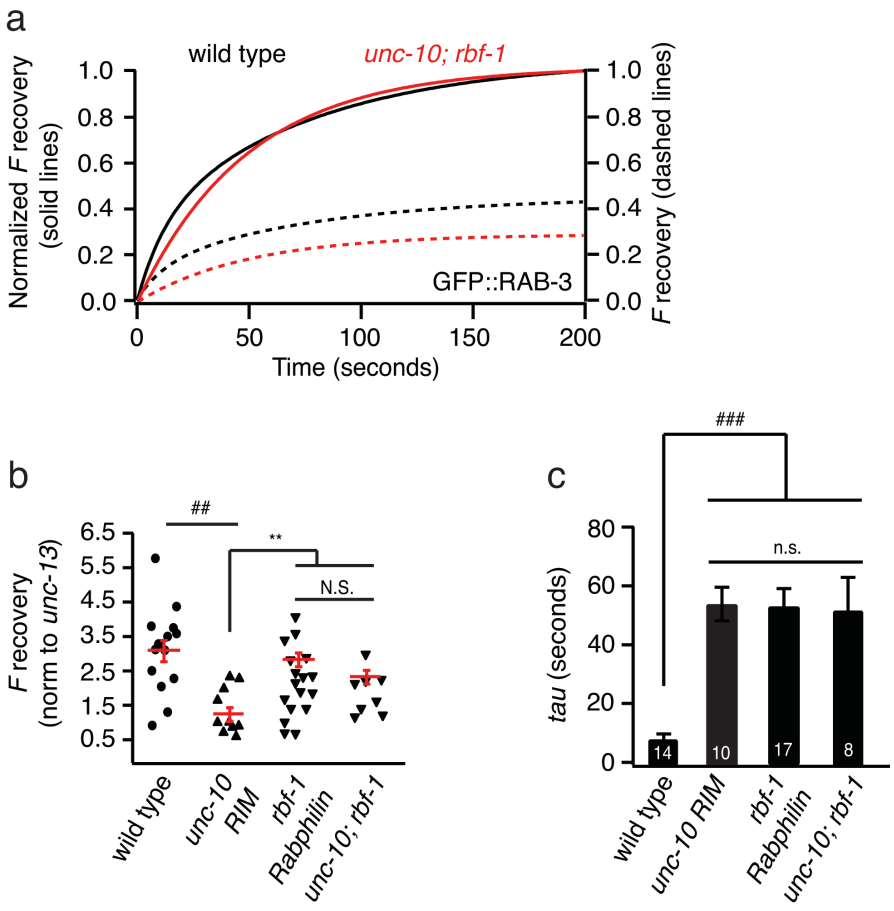


**Figure A.1 Magnitude and rate of RAB-3 recovery in *unc-10; rbf-1* double mutants.** (a) GFP::RAB-3 fitted average fluorescence recovery curves in wild type and *unc-10; rbf-1* double mutants (dashed lines, right axis). Fitted normalized fluorescence recovery curves are also shown (solid lines, left axis). (b) Magnitude of RAB-3 fluorescence recovery (normalized to *unc-13*) at the 50 seconds time point in the indicated genotypes (*unc-10* and *rbf-1* shown for comparison). (c) Tau (τ) values for the kinetic components of RAB-3 exchange in the indicated genotypes (*unc-13*, *unc-10* and *rbf-1* shown for comparison; only $\tau_{fast}$ is shown for wild type). Statistical significance noted as follows: **, $p < 0.01$, compared to *unc-10*; ##, $p < 0.01$, N.S. (not significant), compared to wild type. ###, $p < 0.001$, N.S. (not significant), compared to wild type $\tau_{fast}$ (Student's t-test). The number of worms analyzed for each genotype is indicated. Error bars, standard error of the mean (SEM).

## FUTURE DIRECTIONS

The magnitude but not the rate of RAB-3 exchange in *unc-10; rbf-1* double mutants was similar to that in wild type animals, suggesting that effects of mutating *unc-10* on the magnitude of RAB-3 exchange were eliminated in *unc-10; rbf-1* doubles. Based on our observations we would predict that *unc-10; rbf-1* mutants would have wild type-like mEPSCs. Further experiments are necessary to determine how UNC-10 and RBF-1 act to regulate RAB-3 dynamics. My goal in this Appendix is to highlight the initial observations so that they may be followed up in the future.

## MATERIALS AND METHODS

### Strains

Strains were maintained at 20ºC using standard protocols, on lawns of OP50 for imaging. The following strains were used:

KP6221 *nuIs431* [*punc-129*::GFP::*RAB-3*]

KP7080 *rbf-1(js232) III; nuIs431*

KP6261 *unc-10(md1117) X; Is431*

KP7081 *unc-10(md1117) X; rbf-1(js232) III; nuIs431*

KP6245 *unc-13(s69) I; nuIs431*

KP7082 *nuIs431; ric-7(n2657) V*.

### Fluorescence Imaging and Photobleaching

All quantitative imaging, photobleaching experiments and their analysis was done as previously described (Chapter 2).

## REFERENCES


Alam, A., Schneggenburger, R., & Südhof, T. C. (2005). A Munc13/RIM/Rab3 tripartite complex: from priming to plasticity? *The EMBO Journal*, *24*, 2839–2850.

Barrowman, J., & Novick, P. (2003, November). Three Yips for Rab recruitment. *Nature Cell Biology*, *5*(11), 955–6.

Bastiani, C., & Mendel, J. (2006). Heterotrimeric G proteins in C. elegans. *WormBook*, Oct 13, 1–25.

Basu, J., Betz, A., Brose, N., & Rosenmund, C. (2007). Munc13-1 C1 Domain Activation Lowers the Energy Barrier for Synaptic Vesicle Fusion. *Journal of Neuroscience*, *27*(5), 1200–1210.

Brenner, S. (1974). The genetics of Caenorhabditis elegans. *Genetics*, *77*(1), 71–94.

Castillo, P. E., Janz, R., Südhof, T. C., Tzounopoulos, T., Malenka, R. C., & Nicoll, R. A. (1997). Rab3A is essential for mossy fibre long-term potentiation in the hippocampus. *Nature*, *388*(6642), 590–593.

Ch'ng, Q., Sieburth, D., & Kaplan, J. M. (2008). Profiling Synaptic Proteins Identifies Regulators of Insulin Secretion and Lifespan. *PLoS Genetics*, *4*(11), e1000283.

Chan, C. C., Scoggin, S., Wang, D., Cherry, S., Dembo, T., Greenberg, B., Jin, E. J., Kuey, C., Lopez, A., Mehta, S. Q., Perkins, T. J., Brankatschk, M., Rothenfluh, A., Buszczak, M., & Hiesinger, P. R. (2011). Systematic discovery of Rab GTPases with synaptic functions in Drosophila. *Current Biology*, *21*(20), 1704–1715.

D'Adamo, P., Welzl, H., & Papadimitriou, S. (2002). Deletion of the mental retardation gene Gdi1 impairs associative memory and alters social behavior in mice. *Human Molecular Genetics*, *11*(21), 2567–80.

Dai, Y., Taru, H., Deken, S. L., Grill, B., Ackley, B., Nonet, M. L., & Jin, Y. (2006). SYD-2 Liprin-alpha organizes presynaptic active zone formation through ELKS. *Nature Neuroscience*, *9*(12), 1479–1487.

Deák, F., Shin, O. H., Tang, J., Hanson, P., & Ubach, J. (2006). Rabphilin regulates SNARE-dependent re-priming of synaptic vesicles for fusion. *The EMBO Journal*, *25*(12), 2856–66.

Deng, L., Kaeser, P. S., Xu, W., & Südhof, T. C. (2011). RIM proteins activate vesicle priming by reversing autoinhibitory homodimerization of Munc13. *Neuron*, *69*(2), 317–31.

Dittman, J. S., & Kaplan, J. M. (2006). Factors regulating the abundance and localization of synaptobrevin in the plasma membrane. *Proceedings of the National Academy of Sciences*, *103*(30), 11399–11404.

Dreier, L., Burbea, M., & Kaplan, J. M. (2005). LIN-23-mediated degradation of beta-catenin regulates the abundance of GLR-1 glutamate receptors in the ventral nerve cord of C. elegans. *Neuron*, *46*(1), 51–64.

Feng, W., Liang, T., Yu, J., Zhou, W., Zhang, Y., Wu, Z., & Xu, T. (2012). RAB-27 and its effector RBF-1 regulate the tethering and docking steps of DCV exocytosis in C. elegans. *Science China Life Sciences*, *55*(3), 228–235.

Fukuda, M. (2003). Distinct Rab binding specificity of Rim1, Rim2, rabphilin, and Noc2. *Journal of Biological Chemistry*, *278*(17), 15373–80

Fukuda, M., Kanno, E., & Yamamoto, A. (2004). Rabphilin and Noc2 are recruited to dense-core vesicles through specific interaction with Rab27A in PC12 cells. *Journal of Biological Chemistry*, *279*(13), 13065–75

Garrett, M. D., Zahner, J. E., Cheney, C. M., & Novick, P. J. (1994). GDI1 encodes a GDP dissociation inhibitor that plays an essential role in the yeast secretory pathway. *The EMBO Journal*, *13*(7), 1718–28

Geppert, M., Bolshakov, V. Y., Siegelbaum, S. A., Takei, K., De Camilli, P., Hammer, R. E., & Südhof, T. C. (1994). The role of Rab3A in neurotransmitter release. *Nature*, *369*(6480), 493–497.

Goodwin, P. R., Sasaki, J. M., & Juo, P. (2012). Cyclin-Dependent Kinase 5 Regulates the Polarized Trafficking of Neuropeptide-Containing Dense-Core Vesicles in Caenorhabditis elegans Motor Neurons. *Journal of Neuroscience*, *32*(24), 8158–8172.

Gracheva, E. O., Hadwiger, G., Nonet, M. L., & Richmond, J. E. (2008). Direct interactions between C. elegans RAB-3 and Rim provide a mechanism to target vesicles to the presynaptic density. *Neuroscience Letters*, *444*(2), 137–142.

Graf, E. R., Daniels, R. W., Burgess, R. W., & Schwarz, T. L. (2009). Rab3 dynamically controls protein composition at active zones. *Neuron*, *64*(5), 663–77.

Graf, E. R., Valakh, V., Wright, C. M., Wu, C., Liu, Z., Zhang, Y. Q., & DiAntonio, A. (2012). RIM Promotes Calcium Channel Accumulation at Active Zones of the Drosophila Neuromuscular Junction. *Journal of Neuroscience*, *32*(47), 16586–16596.

Hammarlund, M., Palfreyman, M. T., Watanabe, S., Olsen, S., & Jorgensen, E. M. (2007). Open syntaxin docks synaptic vesicles. *PLoS Biology*, *5*(8), e198.

Han, Y., Kaeser, P. S., Südhof, T. C., & Schneggenburger, R. (2011). RIM Determines $Ca^{2+}$ Channel Density and Vesicle Docking at the Presynaptic Active Zone. *Neuron*, *69*(2), 304–16.

Hao, Y., Hu, Z., Sieburth, D., & Kaplan, J. M. (2012). RIC-7 promotes neuropeptide secretion. *PLoS Genetics*, *8*(1), e1002464.

Hu, Z., Pym, E. C. G., Babu, K., Murray, A. B. V., & Kaplan, J. M. (2011). A Neuropeptide-Mediated Stretch Response Links Muscle Contraction to Changes in Neurotransmitter Release. *Neuron*, *71*(1), 92–102.

Ishikawa-Ankerhold, H. C., Ankerhold, R., & Drummen, G. P. C. (2012). Advanced Fluorescence Microscopy Techniques—FRAP, FLIP, FLAP, FRET and FLIM. *Molecules*, *17*(4), 4047–4132.

Iwasaki, K., Staunton, J., Saifee, O., Nonet, M., & Thomas, J. H. (1997). aex-3 encodes a novel regulator of presynaptic activity in C. elegans. *Neuron*, *18*(4), 613–22.

Jahn, R., & Fasshauer, D. (2012). Molecular machines governing exocytosis of synaptic vesicles. *Nature*, *490*(7419), 201–207.

Janssen, T., Meelkop, E., Lindemans, M., Verstraelen, K., Husson, S. J., Temmerman, L., et al. (2008). Discovery of a cholecystokinin-gastrin-like signaling system in nematodes. *Endocrinology*, *149*(6), 2826–2839.

Kaeser, P. S., Deng, L., Wang, Y., Dulubova, I., Liu, X., & Rizo, J. (2011). RIM Proteins Tether $Ca^{2+}$ Channels to Presynaptic Active Zones via a Direct PDZ-Domain Interaction. *Cell*, *144*(2), 282–95

Kaeser, P., & Südhof, T. (2005). RIM function in short-and long-term synaptic plasticity. *Biochemical Society Transactions*, *33*(6); 1345–9

Kalla, S., Stern, M., Basu, J., Varoqueaux, F., Reim, K., Rosenmund, C., Ziv, N.E., & Brose, N. (2006). Molecular dynamics of a presynaptic active zone protein studied in Munc13-1-enhanced yellow fluorescent protein knock-in mutant mice. *Journal of Neuroscience*, *26*(50), 13054–13066.

Kohn, R. E., Duerr, J. S., McManus, J. R., Duke, A., Rakow, T. L., Maruyama, H., et al. (2000). Expression of Multiple UNC-13 Proteins in the Caenorhabditis elegans Nervous System. *Molecular Biology of the Cell*, *11*(10), 3441–52.

Koushika, S. P., Richmond, J. E., & Hadwiger, G. (2001). A post-docking role for active zone protein Rim. *Nature*, *4*(10), 997–1005.

Lackner, M. R., Nurrish, S. J., & Kaplan, J. M. (1999). Facilitation of Synaptic Transmission by EGL-30 $G_q\alpha$ and EGL-8 PLCβ: DAG Binding to UNC-13 Is Required to Stimulate Acetylcholine Release. *Neuron*, *24*(2), 335–46.

Li, C., Nelson, L. S., Kim, K., & Nathoo, A. (2006). Neuropeptide Gene Families in the Nematode Caenorhabditis elegans. *Annals of the New York Academy of Sciences*, *897*, 239–252.

Lin, C. C., Huang, C. C., Lin, K. H., & Cheng, K. H. (2006). Visualization of Rab3A dissociation during exocytosis: A study by total internal reflection microscopy. *Journal of Cellular Physiology*, *211*(2), 316–26.

Lonart, G., Janz, R., Johnson, K. M., & Südhof, T. C. (1998). Mechanism of action of rab3A in mossy fiber LTP. *Neuron*, *21*(5), 1141–1150.

Madison, J. M., Nurrish, S., & Kaplan, J. M. (2005). UNC-13 interaction with syntaxin is required for synaptic transmission. *Current Biology*, *15*(24), 2236–2242.

Mahoney, T. R. (2006). Regulation of Synaptic Transmission by RAB-3 and RAB-27 in Caenorhabditis elegans. *Molecular Biology of the Cell*, *17*(6), 2617–2625.

McEwen, J. M., Madison, J. M., Dybbs, M., & Kaplan, J. M. (2006). Antagonistic regulation of synaptic vesicle priming by Tomosyn and UNC-13. *Neuron*, *51*(3), 303–15.

Miller, K. G., Emerson, M. D., & Rand, J. B. (1999). $G_o\alpha$ and Diacylglycerol Kinase Negatively Regulate the $G_q\alpha$ Pathway in C. elegans. *Neuron*, *24*(1) 231–242.

Mollard, von, G. F., & Mignery, G. A. (1990). rab3 is a small GTP-binding protein exclusively localized to synaptic vesicles. *Proceedings of the National Academy of Sciences*, *87*(5), 1988–92.

Mollard, von, G. F., Südhof, T. C., & Jahn, R. (1991). A small GTP-binding protein dissociates from synaptic vesicles during exocytosis. *Nature*, *349*(6304), 79–81

Moreira, J. E., Llinás, R. R., & Fukuda, M. (2008). Role of Rab27 in synaptic transmission at the squid giant synapse. *Proceedings of the National Academy of Sciences*, *105*(41), 16003–8

Mueller, V. J., Wienisch, M., Nehring, R. B., & Klingauf, J. (2004). Monitoring clathrin-mediated endocytosis during synaptic activity. *Journal of Neuroscience*, *24*(8), 2004–2012.

Muller, M., Liu, K. S. Y., Sigrist, S. J., & Davis, G. W. (2012). RIM Controls Homeostatic Plasticity through Modulation of the Readily-Releasable Vesicle Pool. *Journal of Neuroscience*, *32*(47), 16574–16585.

Muller, M., Pym, E., Tong, A., & Davis, G. W. (2011). Rab3-GAP controls the progression of synaptic homeostasis at a late stage of vesicle release. *Neuron*, *69*(4), 749–62.

Neher, E. (2010). What is Rate-Limiting during Sustained Synaptic Activity: Vesicle Supply or the Availability of Release Sites. *Frontiers in Synaptic Neuroscience*, *2*, 144.

Neher, E., & Sakaba, T. (2008). Multiple Roles of Calcium Ions in the Regulation of Neurotransmitter Release. *Neuron*, *59*(6), 861–872.

Nonet, M. L., Staunton, J. E., Kilgard, M. P., Fergestad, T., Hartwieg, E., Horvitz, H. R., et al. (1997). Caenorhabditis elegans rab-3 Mutant Synapses Exhibit Impaired Function and Are Partially Depleted of Vesicles. *The Journal of Neuroscience*, *17*(21), 8061–73.

Nurrish, S., Ségalat, L., & Kaplan, J. M. (1999). Serotonin inhibition of synaptic transmission: $G\alpha_o$ decreases the abundance of UNC-13 at release sites. *Neuron*, *24*(1), 231–42.

Okamoto, M., Schmitz, F., Hofmann, K., & Sudhof, T. C. (1997). Rim is a putative Rab3 effector in regulating synaptic-vesicle fusion. *Nature*, *388*(6642), 593–598.

Pavlos, N. J., Grønborg, M., Riedel, D., Chua, J. J. E., Boyken, J., Kloepper, T. H., et al. (2010). Quantitative analysis of synaptic vesicle Rabs uncovers distinct yet overlapping roles for Rab3a and Rab27b in $Ca^{2+}$-triggered exocytosis. *Journal of Neuroscience*, *30*(40), 13441–13453.

Peled, E. S., & Isacoff, E. Y. (2011). Optical quantal analysis of synaptic transmission in wild-type and rab3-mutant Drosophila motor axons. *Nature Neuroscience*, *14*(4), 519–26.

Richmond, J. E., & Broadie, K. S. (2002). The synaptic vesicle cycle: exocytosis and endocytosis in Drosophila and C. elegans. *Current Opinion in Neurobiology*, *12*(5), 499–507.

Richmond, J. E., & Jorgensen, E. M. (1999). One GABA and two acetylcholine receptors function at the C. elegans neuromuscular junction. *Nature Neuroscience*, *2*(9), 791–7.

Richmond, J. E., Davis, W. S., & Jorgensen, E. M. (1999). UNC-13 is required for synaptic vesicle fusion in C. elegans. *Nature Neuroscience*, *2*(11), 959–64.

Rosenmund, C., Sigler, A., Augustin, I., Reim, K., Brose, N., & Rhee, J.-S. (2002). Differential control of vesicle priming and short-term plasticity by Munc13 isoforms. *Neuron*, *33*(3), 411–424.

Sakane, A., Manabe, S., Ishizaki, H., Tanaka-Okamoto, M., Kiyokage, E., Toida, K., et al. (2006). Rab3 GTPase-activating protein regulates synaptic transmission and plasticity through the inactivation of Rab3. *Proceedings of the National Academy of Sciences*, *103*(26), 10029–10034.

Schlüter, O. M, Schmitz, F., Jahn, R., Rosenmund, C., & Südhof, T. C. (2004). A complete genetic analysis of neuronal Rab3 function. *The Journal of Neuroscience*, *24*(29), 6629–37.

Schlüter, O. M., Basu, J., & Südhof, T. C. (2006). Rab3 superprimes synaptic vesicles for release: implications for short-term synaptic plasticity. *The Journal of Neuroscience*, *26*(4), 1239–46.

Schoch, S., Castillo, P. E., Jo, T., & Mukherjee, K. (2002). RIM1alpha forms a protein scaffold for regulating neurotransmitter release at the active zone. *Nature*, *415*(6869), 321–6.

Sieburth, D., Ch'ng, Q., Dybbs, M., Tavazoie, M., Kennedy, S., Wang, D., et al. (2005). Systematic analysis of genes required for synapse structure and function. *Nature*, *436*(7050), 510–517.

Simon, D. J., Madison, J. M., & Conery, A. L. (2008). The microRNA miR-1 regulates a MEF-2-dependent retrograde signal at neuromuscular junctions. *Cell*, *133*(5), 903–15.

Stahl, B., Chou, J. H., Li, C., Südhof, T. C., & Jahn, R. (1996). Rab3 reversibly recruits rabphilin to synaptic vesicles by a mechanism analogous to raf recruitment by ras. *The EMBO Journal*, *15*(8), 1799–809.

Stahl, B., Mollard, von, G. F., Walch-Solimena, C., & Jahn, R. (1994). GTP cleavage by the small GTP-binding protein Rab3A is associated with exocytosis of synaptic vesicles induced by alpha-latrotoxin. *Journal of Biological Chemistry*, *269*(40), 24770–6.

Star, E. N. (2005). Real-time imaging of Rab3a and Rab5a reveals differential roles in presynaptic function. *The Journal of Physiology*, *569*(1), 103–117.

Staunton, J., Ganetzky, B., & Nonet, M. L. (2001). Rabphilin potentiates soluble N-ethylmaleimide sensitive factor attachment protein receptor function independently of rab3. *The Journal of Neuroscience*, *21*(23), 9255–64.

Stigloher, C., Zhan, H., Zhen, M., Richmond, J., & Bessereau, J.-L. (2011). The presynaptic dense projection of the Caenorhabditis elegans cholinergic neuromuscular junction localizes synaptic vesicles at the active zone through SYD-2/liprin and UNC-10/RIM-dependent interactions. *Journal of Neuroscience*, *31*(12), 4388–4396.

Südhof, T. C. (2004). The synaptic vesicle cycle. *Annual Review of Neuroscience*, *27*, 509–547.

Südhof, T. C. (2012). The presynaptic active zone. *Neuron*, *75*(1), 11–25.

Sudhof, T. C., & Rizo, J. (2011). Synaptic Vesicle Exocytosis. *Cold Spring Harbor Perspectives in Biology*, *3*(12), a005637.

Tsuboi, T., & Fukuda, M. (2005). The C2B domain of rabphilin directly interacts with SNAP-25 and regulates the docking step of dense core vesicle exocytosis in PC12 cells. *The Journal of Biological Chemistry*, *280*(47), 39253–39259.

Tsuboi, T., & Fukuda, M. (2006). Rab3A and Rab27A cooperatively regulate the docking step of dense-core vesicle exocytosis in PC12 cells. *Journal of Cell Science*, *119*(11), 2196–203.

Wang, X., Wang, Q., Yang, S., & Bucan, M. (2011). Impaired Activity-Dependent Plasticity of Quantal Amplitude at the Neuromuscular Junction of Rab3A Deletion and Rab3A Earlybird Mutant Mice. *The Journal of Neuroscience*, *31*(10), 3580–8.

Wang, Y., & Südhof, T. C. (2003). Genomic definition of RIM proteins: evolutionary amplification of a family of synaptic regulatory proteins. *Genomics*, *81*(2), 126–137.

Weimer, R. M., Gracheva, E. O., & Meyrignac, O. (2006a). UNC-13 and UNC-10/Rim Localize Synaptic Vesicles to Specific Membrane Domains. *Journal of Neuroscience*, *26*(31), 8040–8047.

Weimer, R. M. (2006b). Preservation of C. elegans tissue via high-pressure freezing and freeze-substitution for ultrastructural analysis and immunocytochemistry. *Methods in Molecular Biology*, *351*, 203–221.

Xiao, Z., Jaiswal, M. K., Deng, P.-Y., Matsui, T., Shin, H.-S., Porter, J. E., & Lei, S. (2011). Requirement of phospholipase C and protein kinase C in cholecystokinin-mediated facilitation of NMDA channel function and anxiety-like behavior. *Hippocampus*, *22*(6), 1438–1450.

Xue, L., & Mei, Y. (2011). Synaptic vesicle recycling at the calyx of Held. *Acta Pharmacologica Sinica*, *2*(3), 280–287.

Yang, Y., & Calakos, N. (2011). Munc13-1 Is Required for Presynaptic Long-Term Potentiation. *Journal of Neuroscience*, *31*(33), 12053–12057.

Zhang, J., Schulze, K. L., Hiesinger, P. R., Suyama, K., Wang, S., Fish, M., Acar, M., Hoskins, R. A., Bellen, & H. J., Scott, M. P. (2007). Thirty-one flavors of Drosophila rab proteins. *Genetics*, *176*(2), 1307–1322.